Tectonic controls on residual oil saturation below the present-day fluid contact level in reservoirs of the Persian Gulf

E. Heydari-Farsani[1,*], J. E. Neilson[1], G. I. Alsop[1], H. Hamidi[2]

[1]School of Geosciences, King's College, University of Aberdeen, Aberdeen, AB24 3UE, UK

[2]School of Engineering, King's College, University of Aberdeen, Aberdeen AB24 3UE, UK

Abstract

The presence of residual oil below the present-day free water level (FWL) and oil water contact (OWC) is common in many oil fields in the Middle East, particularly those in the Persian Gulf. This residual oil is seen in both clastic and carbonate reservoirs prior to the start of production. The characterisation and modelling of these fields is difficult in practice. Also, these residual oils below the FWL and OWC could become classified as reserves if ways to produce them could be found. However, the first step is to better understand their origin. Therefore, the goal of this study was to investigate the role of geological events on the presence of the residual oil zone (ROZ) below the FWL and OWC.

It has been suggested that the presence of residual oil below the present day FWL and OWC is related to the geotectonic history of the region. From the middle Miocene, reverse faulting and overfolding propagated over the Zagros, leading to the amplification of folds and the migration of the Zagros orogeny towards its foreland basin (Persian Gulf). In response to this additional massive loading on the continental margin, the forebulge amplitude was increased, its location migrated towards the uplifted Zagros Mountains, and consequently the Persian Gulf became narrower. This exerted a north to north-east downward tilting of the entire basin, including all the structures and reservoirs previously filled by hydrocarbons. This basin tilting

changed the equilibrium of the structures and their fluid contents, and resulted in the hydrocarbons and water attempting to find a new equilibrium. Under these conditions, the early migrated and accumulated oil was flushed out by water (imbibition), and a ROZ was left below the present day FWL and OWCs. The angle of regional basin tilt has been calculated to be 0.836° based on seismic sections.

Keywords: Residual oil below fluid contact, Zagros collision, Persian Gulf, foreland basin, regional tilting

1. Introduction

The Persian Gulf, which is situated at the centre of the Middle East, is the location of remarkable hydrocarbon reservoirs. Many of these reservoirs present a thickness of residual oil below the free water level (FWL) and oil water contact (OWC) prior to the start of production (Figure 1). This residual oil is seen in both carbonate and clastic reservoirs, and in many of them increases towards the northern parts of the fields (Figure 1). Breached and reformed seal, tilted fluid contact due to hydrodynamic aquifer and regional or local basin tilt are the main processes that generate residual oil below the FWL and OWC (Melzer et al., 2006). The characterisation and modelling of reservoirs with residual oil below the FWL and OWC, prior to the start of production, is difficult. Also, these significant reserves of oils occur below the FWL and OWC if ways to produce them can could be found. The first step, however, is to better understand their origin. Therefore, the goal of this study was to improve our understanding of the role of geological events on the presence of residual oil below the FWL and OWC by introducing a new geological model for the Persian Gulf region.

Geological studies have been a fundamental part of exploration and production projects since the beginning of the oil industry in the Persian Gulf. The sedimentology of the Persian Gulf was first studied by Emery (1956), although a better understanding of sediment generation

48 processes and the pattern of sediment accumulation was heralded by the publication of *The*
49 *Persian Gulf* (Purser, 1973). In addition to these key studies, several others have contributed
50 to our understanding of the geology of the Zagros and its foreland basin (Persian Gulf),
51 including James and Wynd (1965), Mina et al. (1967), Dunnington (1974), Falcon (1974),
52 Setudehnia (1978), Szabo and Kheradpir (1978), Murris (1980), Koop and Stoneley (1982),
53 Beydoun et al. (1992), Motiei (1995), Alsharhan and Nairn (1997), Uchupi et al. (1999),
54 Swift and Ross (2002), Homke et al. (2004), Nadjafi et al. (2004), Vazirimoghaddam et al.
55 (2006) and Khadivi et al. (2010), which have all demonstrated the stratigraphy of different
56 parts of the Zagros and the Persian Gulf. In addition, Ala et al. (1980), Ala (1982), Bordenave
57 and Burwood (1990), Ghasemi-Nejad et al. (2009) and Abdollahifard et al. (2011)
58 specifically studied the petroleum geology of the Zagros and the Persian Gulf.

59 Alavi and Mahdavi (1994), Ehsanbakhsh (1996), Nazari and Shahidi (1998), Karimi-
60 Bavandpour (1999), Talebian (1999), Mohajjel and Fergusson (2000) and Alavi (2004)
61 carried out extensive geological mapping in different parts of the Zagros and the Persian
62 Gulf, and have contributed a better understanding of the development of the Zagros Belt and
63 Persian Gulf Basin. The tectonostratigraphy of the Zagros has been studied by Alavi (1996),
64 Sherkati et al. (2006), Mouthereau et al. (2007), Homke et al. (2009, 2010).

65 Stocklin (1968), Falcon (1974), Colman-Sadd (1978), Bahroudi and Koyi (2003, 2004),
66 McQuarrie (2004), Sherkati and Letouzey (2004), Sepehr and Cosgrove (2004), Molinaro et
67 al. (2005), Lacombe et al. (2006, 2007), Mouthereau et al. (2007), Aubourg et al. (2008) and
68 Jahani et al. (2009) addressed the structural geology of different parts of the Zagros, whilst
69 Vergas et al. (2011) integrated geological and geophysical data to produce a crustal cross-
70 section of the NW Zagros.

71 The fracture pattern and stress direction in the Zagros have been reported on by Lacombe et
72 al. (2011), and the link between the closure of the Neo-Tethys and the generation of the
73 Zagros has been investigated by Braud and Brunn (1977), Alavi (1980), Berberian and King
74 (1981), Dercourt et al. (1986), Sengör et al. (1988), Dercourt et al. (1993), Alavi (1994),
75 Stampfli and Borel (2002), Agard et al. (2005) and Hafkenscheid et al. (2006).

76 Tavani et al. (2011) presented deformation pattern of the SW Zagros anticlines. The salt
77 diapirism in the Zagros and adjacent area have been studied by Kent (1958), Falcon (1969),
78 Talbot and Jarvis (1984), Alavi (1994) and Talbot and Alavi (1996).

79 Faghih and Sarkarinejad (2011) demonstrated ductile deformation in the Sanandaj Sirjan
80 Zone of the Zagros, whilst Allen and Talebian (2011) investigated the fault patterns in the
81 Dezful Embayment, concluding that ophiolite obduction in the Late Cretaceous played an
82 important role in the stratigraphy of the Zagros.

83 Stöcklin (1968, 1974), Berberian and King (1981), Yilmaz (1993), Alavi (1994), Hooper et
84 al. (1994), Jolivet and Faccenna (2000), Robertson (2000), Fergusson and Sahandi (2003),
85 McQuarrie et al. (2003), Agard et al. (2005), Vincent et al. (2005), Ghasemi and Talbot
86 (2006), Ghalamghash et al. (2009), Mazhari et al. (2009) and Ballato et al. (2010)
87 investigated the time of the collision between the Arabian and Iranian plates, and the position
88 of the collision suture has been demonstrated by Stöcklin (1968), Ricou et al. (1977), Alavi
89 (1994), Agard et al. (2005, 2006), Paul et al. (2006) and Shafaii Moghadam et al. (2010).

90 Alavi (1996, 1980, 2004, 2007), Koop et al. (1982), Husseini (1989), Talbot and Alavi
91 (1996), Bahroudi and Koyi (2003), Agard et al. (2005, 2011), Sherkati et al. (2006), Homke
92 et al. (2009), Pirouz et al. (2011), Moutherean (2011) and Verdal (2011) analysed the
93 geodynamic evolution of the Zagros through time.

Studies on residual oil have mostly focused on the remaining and residual oil in the transition zone, not below the FWL or OWC.

Kirkham et al. (1996) suggested that presence of residual oil could be related to the Zagros mountains although didn't prove it. Mezler et al. (2006) and Koperna et al. (2006) reported significant oil reserves in the residual oil zones (ROZs) of the Permian Basin, USA. The production characteristics of ROZs have been reported on by Parker and Rudd (2000, Middle East reservoirs), Koperna et al. (2006) and Harouaka et al. (2013; Permian Basin reservoirs, USA). Pelissier et. al. (1980) studied the hydrodynamic activity in some of the Middle East reservoirs. Thomasen and Jacobsen (1994) and Vejbaek et al. (2005) evaluated the relationship between active hydrodynamic drive and the presence of ROZs in North Sea reservoirs, and Aleidan at al. (2017) carried out a palaeo-oil characterisation and fundamental analysis of the ROZ for a field in Saudi Arabia.

2. Field descriptions

Three fields, located in the east, centre and west of the Persian Gulf, were selected for petrophysical evaluation, and an investigation of the residual oil observed (Figure 1). Due to matters of confidentiality, these fields are referred to throughout as A (east), B (central) and C (west).

- Field A forms an elongated NNE–SSW anticlinal structure (Figure 1). It is located in the eastern part of an intrashelf basin within the Arabian continental shelf that developed during the middle Cretaceous (Jordan et al., 1985; Alsharhan and Nairn, 1997; Ziegler, 2001). Within this intrashelf basin, the Khatiyah Formation (Fm) facies (end of the Early Cretaceous) was deposited under anoxic conditions, with the organic matter preserved turning the Khatiyah Fm facies into a source rock. This intrashelf

basin is surrounded by concentric shelf facies belts, including fore-shoal, shoal, back shoal and protected platform facies, corresponding to the Cenomanian–Turonian Sarvak (Mishrif) Fm, which forms the reservoir. The overall progradation of these facies has created a petroleum system in which the carbonate reservoirs of the Sarvak Fm overlie the source rocks of the Khatiyah Fm (Farzadi, 2006). The seal to the Sarvak (Mishrif) reservoir is provided by 2–5 m of overlying Coniacian Laffan Fm shale (Farzadi, 2006).

- Field B is located in the centre of the Persian Gulf (Figure 1). The field is a gentle domal anticline, trending NNE–SSW, with flanks dipping 1–3°. The oil is produced from three carbonate reservoirs of Late Jurassic to middle Cretaceous age. These reservoirs are the Sarvak (Mishrif) Fm of Cenomanian–Turonian age, the Dariyan (Shuaiba) Fm of Aptian age and the Surmeh Fm (Arab Members A1 and C) of Kimmeridgian–Tithonian age. The carbonate Sarvak (Mishrif) Fm of this field was selected to be incorporated in the study. The seal to the Sarvak (Mishrif) Fm is provided by 20–30 m of overlying Coniacian Laffan Fm shale (Farzadi, 2006).
- Field C is located in the NW Persian Gulf (Figure 1). The structure is an elongated NNE–SSW anticline. The oil is produced from three carbonate and one sandstone reservoirs. The carbonate reservoirs include the Dariyan (Shuaiba) Fm of Aptian age, the Gadvan (Kharaib) Fm of Barremian to Aptian age and the Fahlyian (Yamama) Fm of Berriasian–Valanginian age. The clastic reservoir that was selected to be incorporated in this study is the Albian Sand B of the Kazddumi (Burgan) Fm, which was deposited in a deltaic environment. This reservoir was selected to make sure the ROZ was studied in both carbonate and clastic reservoirs. The seal to the reservoir is provided by almost 50 m of overlying Kazhdumi shale.

3. Available data

142 The following data were used in this study:

143 • Petrophysical and reservoir data: These data were mainly used to generate computer
144 processing interpretation (CPI) logs to determine the OWC depth, the water and oil
145 saturation and to confirm the presence of the residual oil below the FWL and OWC. A
146 large set of wireline and logging while drilling logs (GR, NPHI, RHOB, DT, SP,
147 RXO and RT) were available, although no nuclear magnetic resonance data exist for
148 these fields. All available logs were inspected and quality checked to make sure only
149 valid data were used. Petrophysical interpretations were carried out on more than 90
150 wells, using final quality checked logs, conventional core analysis and special core
151 analysis.
152 • Formation pressure data for before the start of production were available for a limited
153 number of wells for Fields A and C. These were used to define the FWL depth. There
154 is only one well in fields A and C with pressure data in the aquifer.
155 • Drill stem tests (DSTs), core oil-staining and mud-logging gas chromatography
156 (methane, ethane, propane and total gas) were used in conjunction with the CPIs to
157 define the depth of the OWC and to investigate whether residual oil was present
158 below the present-day contact.
159 • Geological data and studies: A comprehensive literature review was carried out, and
160 the stratigraphy, tectonics, depositional environment and petroleum geology were
161 analysed and integrated with the petrophysical results to present a model for the
162 presence of residual oil below the FWL and OWC. A summary of this study is
163 presented in Section 5.
164 • Geophysical data: Seismic lines were used to investigate and calculate the subsidence,
165 tilting and flexural loading of the Persian Gulf Basin.

4. Fluid contact determination

The FWL is the level at which the capillary pressure (pressure of the non-wetting phase – pressure of the wetting phase) is zero (Spinler and Baldwin, 1999; Darling, 2005; Tiab and Donaldson, 2015). In theory, it is a potentiometric surface, best determined using pressure data to define the intersection between the hydrocarbon zone gradient and the water zone gradient on a formation pressure vs. depth crossplot (Tiab and Donaldson, 2015). Above the FWL, where the capillary pressure is not zero, hydrocarbons can displace water.

The OWC is the point at which the water saturation (Sw) is 100% (in theory), and the capillary pressure is not zero (Spinler and Baldwin, 1999; Darling, 2005; Tiab and Donaldson, 2015). The OWC is apparent on well logs, in cores (by oil-staining) and in mud-logging gas data (Tiab and Donaldson, 2015). At the OWC, the hydrocarbon saturation starts to increase upwards from some minimum (Elshahawi et al., 1999).

In rocks with poor reservoir quality (small pore throat size and low permeability), a certain entry pressure is required before the value of Sw can fall below unity. Once this pressure is reached, hydrocarbons will be found in the rock (Darling, 2005).

In reservoirs with good reservoir quality (i.e. all reservoirs in the studied fields with an average permeability of 10–200 mD), the FWL and OWC occur at close depths (Darling, 2005; Tiab and Donaldson, 2015). In this study therefore, ‘fluid contact’ is used as a general term to describe where the FWL and OWC cannot be resolved or have a similar depth. The FWL, OWC, oil down to (ODT) and water up to (WUT) were defined for more than 90 wells in the studied fields, with special attention being paid to the early wells that were drilled prior to the start of production.

Field A has a FWL at 2900 m TVDSS, obtained from the formation pressure data (Figure 2A). There are also three preproduction wells located in the north and south of the field that display OWCs (determined mainly from log data) with almost similar depths (Figure 3A). The northernmost well (A4) in this field has a WUT at 2912 m TVDSS.

Field B has an OWC at 1221 m TVDSS, based on data from five wells located in different parts of the field. There is no formation pressure data for this field (Figure 3B).

Field C illustrates a FWL at 2337 m TVDSS, determined by extrapolation of the formation pressure data (Figure 2B) from a well located in the south of the field (Figure 3C). The depth of this FWL is supported by the ODT and WUT seen in a well drilled on the northern flank of the field (Figure 3C). The ODT is apparent above a shaley interval at 2334 m TVDSS, and the WUT is located 10 m deeper, at 2343 m TVDSS (Figure 3C). Therefore, the OWC depth in the northern flank is located between 2334 and 2343 m TVDSS, very close to the FWL depth seen in the southern parts of the field.

Based on the petrophysical interpretation and fluid contact determination performed in the studied fields, the following significant observations were made:

1- The present-day FWL and OWC in these fields do not correspond to 100% Sw, but to 50–60% Sw in some areas of Field A, 80% Sw in some areas of Field B and 75% Sw in some areas of Field C (Figures 3). This indicates that there is a ROZ below the present-day FWL and OWC in all three fields.

2- The presence of residual oil below the present-day FWL and OWC is predominantly seen in the northern parts of the fields, rather than the southern parts (Figures 1, 3), regardless of lithology.

3- No tilting of the fluid contact was observed in the early wells in the studied fields

(Figure 3). The FWL and OWCs depths show minimum deviation across Fields A and C. A similar observation was made for Field B using the OWC depths in the early wells.

5. Regional geology

The regional geology of the Persian Gulf and surrounding area was investigated to explore the possible effect of geological events on the natural water flooding and presence of residual oil below the FWL and OWC. Special attention was paid to basin analysis and its relationship to oil generation in the source rock, its migration to the reservoir, the structural history and possible further changes in the fluid equilibrium. A summary of regional geology and main events are shown in Figure 4.

The Persian Gulf is part of the Arabian continental plate. The petroleum geology of the Arabian Plate has been controlled by the various tectonic activities; in the Persian Gulf, the Zagros collision has played the major role.

The Zagros Fold-thrust Belt has been defined as a NW–SE-trending orogeny, extending for about 1800 km from the East Anatolian Fault in eastern Turkey (45°E, 36°E) to the Makran Subduction Zone in southern Iran (26°N, 58°E) (Mouthereau et al., 2012).

The sediments drilled by the wells and evident in outcrops show the evolution of 10 km of deposits, from the passive margin to the active margin and foreland basin in the Zagros and the Persian Gulf Basin (Morris, 1977).

5.1 Passive margin

During the Late Permian to Middle Triassic, a new passive margin developed after the opening of the Neo-Tethys Ocean (Ziegler, 2001). The sediments of this passive margin

deposited in an equatorial shallow-platform sea. This passive margin continued until the end of the Mesozoic, and its sediments form 5 km of alternating carbonate, siliciclastic and evaporitic deposits (Homke et al., 2004; Sherkati and Letouzey, 2004; Farzipour-Saein et al., 2009). The majority of the source rock and hydrocarbon reservoir formations of the Middle East were deposited in this passive margin, including the Khatiyah (source rock in Fields A and B), Sarvak (reservoir in Fields A and B) and Kazhdumi (source rock and reservoir in Field C) Fms in the studied fields.

5.2 Generation of the foreland basin

Many of the anticlinal structural traps in the Persian Gulf (including those of Fields A–C) were the result of doming of the underlying Cambrian Hormuz salt prior to the Turonian and the deposition of the Sarvak (Mishrif) and Kazhdumi Fms (Arian and Noroozpour, 2015).

Following the generation of the anticlinal structures, the Neo-Tethys Ocean continued to close due to the continuous subduction of the Afro–Arabian Plate beneath the Eurasian Plate (Alavi, 2004; Mouthereau et al., 2012). As a result of this subduction, in the Eocene (between 55 and 37 Ma), a magmatic flare-up occurred in the Uromieh Dokhtar Magmatic Arc (Vincent at al., 2005; Agard et al., 2011; Verdel et al., 2011). Magmatism in the UDMA ceased before the start of collision in various parts of the Zagros in the Oligo–Miocene (Chung et al., 2010 in Agard et al., 2011).

At the same time, beginning in the late Turonian and occurring through the Late Campanian/Early Maastrichtian, oceanic sedimentary prisms and ophiolite masses were overthrust and glided onto the edge of the Arabian shelf from NW Syria to SE Oman (Beydoun et al., 1992).

255 The crustal thickening associated with the tectonic evolution in the NE of the Persian Gulf
256 caused the lithosphere to bend, resulting in the development of a foreland basin (foredeep)
257 and its associated forebulge to the south and SW of the Zagros. This foreland basin is about
258 2000 km in length (Hail-Gaara Arch to Zendan-Minab Fault Zone) and some 250 to 350 km
259 in width. It includes the terrestrial Mesapotamia Basin in Iraq and the Persian Gulf (Figure 1).

260 Foreland basins are the elongated sedimentary basins located on continental lithosphere at the
261 outer edges of mountain belts (Dickinson, 1974). The distal margin of a foreland basin is
262 defined by the forebulge, which is a small uplift, formed by the strength and resistance of the
263 lithosphere in reaction to the loading caused by folding and thrusting (Dickson, 1974 and
264 Miall, 2010). There is evidence that the forebulge can migrate across a foreland basin, both
265 towards and away from the thrust and fold belt, and that it may, in some cases, act as a
266 localised sediment source (DeCelles and Giles, 1996).

267 While emplacement of the Neo-Tethyan ophiolites onto the Afro–Arabian Plate was ongoing
268 during the Campanian–Early Maastrichtian (Alavi, 2004), in the Zagros and Persian Gulf
269 area, deposition of the Ilam and Gurpi Fms occurred (Figure 5). In the northern part of the
270 Persian Gulf, closer to the Zagros front, sandstones and conglomerates of the Amiran Fm are
271 present, which were sourced from the erosion of ophiolite wedges (James and Wynd, 1965;
272 Mouthereau et al., 2012).

273 During the Eocene, the Kashgan, Shahbazan, Pabdeh and Jahrum Fms were deposited in the
274 Persian Gulf foreland basin (Figure 5), while continued thrust stacking and ophiolite
275 emplacement were the major events of the progressive deformation (Alavi, 2004). This
276 period of deposition was followed by a hiatus in sedimentation in the area. This may have
277 been the result of uplift of the Arabian continental margin, following the sedimentation of the

278 Kashkan, Shahbazan, Pabdeh and Jahrum Fms, but prior to a marine transgression and
279 deposition of the Asmari Fm.

280 **5.3 Hydrocarbon generation and the filling of structures**

281 The crustal thickening associated with the tectonic evolution of the Zagros provided a huge
282 sediment supply to the basin. As a result of this massive sediment supply and the increasing
283 burial of older formations, the Kazhdumi (Middle Albian) and Khatiyah (Upper Albian) Fms,
284 which are the source rocks of the studied fields, entered the oil window in the Eocene around
285 39 Ma, during deposition of the Pabdeh Fm. Oil generation continued, and then the oil
286 migrated to the reservoirs. The fluid connection between the source rock and the reservoir
287 was facilitated by faults and fractures (Bordenave, 2002). Based on geochemical and burial
288 history studies, the oil migration was complete by the Late Eocene/Early Oligocene. At this
289 time, it is assumed that the structures were completely filled with oil, from the crest to the
290 fluid contact or spill point.

291 **5.4 Collision and Persian Gulf Basin tilting**

292 Figure 5 shows the sedimentation of different formations in the Persian Gulf foreland basin,
293 from the Turonian to the Miocene. The location of one of the studied fields (B) is also shown.

294 The Zagros collision was initiated in the Late Eocene–Early Oligocene (Mouthereau et al.,
295 2012). However, the elevation, uplift and exposure of older sediments started later, in the
296 Miocene (Emami, 2008; Khadivi et al., 2012; Mouthereau et al., 2012). At 15 Ma, folding
297 began in the northern parts of the Zagros, and then propagated southwards after 12 to 11 Ma
298 (Emami, 2008; Khadivi et al., 2012). Numerous thrust faults and folds were generated in an
299 area around 300 km wide. As a result of this deformation, a shortening of 40 to 70 km
300 occurred in the Zagros area (Sherkati and Letouzey, 2004; Molinaro et al., 2005). This crustal
301 shortening and thickening resulted in the uplift of the Zagros region.

302 The Early Miocene witnessed a significant change in the direction of plate motion, from NE
303 to north. This occurred following rifting in the Red Sea (McQuarrie et al., 2003; Arrajehi et
304 al., 2010) and the westward opening of the Gulf of Aden (Leroy, 2004).

305 From the Middle Miocene, the Zagros Mountains developed their present shape, reaching a
306 height of more than 4548 m. Reverse faulting and overfolding propagated over the Zagros,
307 reaching the foreland basin, and leading to the amplification of folds and the migration of the
308 Zagros Orogeny towards its foreland basin.

309 In response to this additional massive loading on the continental margin, the forebulge
310 amplitude increased, and its location moved towards the uplifted Zagros (Alavi, 2004)
311 (Figure 6). As a result of this forebulge movement, the Persian Gulf foreland basin migrated
312 towards the orogenic suture (Alavi, 2004), becoming narrower (Figure 6). This would have
313 exerted a north to NE downward tilt of the entire basin, including all the structures and
314 reservoirs filled by hydrocarbons, from the crest to the fluid contact or spill point. The
315 location of Field B, before and after the tectonic subsidence, is shown with dashed and solid
316 rectangles, respectively, in Figure 6.

317 The erosion of the uplifted rocks may have generated sufficient sediments for the deposition
318 of the 3000-m-thick regressive siliciclastic sequence of the Razak, Guri, Gachsaran, Mishan,
319 Aghajari and Bakhtiyari Fms in different parts of this narrower compressional basin (Figure
320 7). These sediments display distinctive lateral and vertical facies variations, and were affected
321 by various tectonic events. The younger formations comprise coarsening-upward flysch and
322 molasse sequences, and display a continuation of the progradation of sediments sourced from
323 the Zagros towards the SW through time.

324 **6. Discussion of residual oil below present-day fluid contacts**

Prior to the start of reservoir production, residual oil below the FWL and OWC generally occurs because of the natural and geological water flooding of an oil reservoir (O'Sullivan et al., 2010; Aliedan et al., 2016). The main processes that generate ROZs below fluid contacts are (Melzer et al., 2006):

- Breaching and reforming of the seal;
- Tilted fluid contact due to hydrodynamic aquifer; and
- Regional or local basin tilt.

Breaching and reforming of the seal. Breaching of the seal occurs as a result of tectonic forces or due to the hydrocarbon column height being sufficient to break the seal (O'Sullivan et al., 2010). In this case, hydrocarbons partially escape from the reservoir and, if the new oil column is significantly less than the original one, a thickness of residual oil will occur below the remaining oil as basinal water moves up into the oil-depleted interval (Figure 8A). If seal failure happens, a constant thickness of the ROZ is seen below the remaining oil across the entire field (Figure 8A).

As mentioned earlier, residual oil below the present-day fluid contact is not uniformly found across all the studied fields; it is mainly seen in the northern parts of the studied fields (Figures 1 and 3). This option for the presence of the residual oil below the present-day fluid contact in these fields can therefore be discounted.

Tilted fluid contact due to hydrodynamic aquifer. A change in the hydrodynamic conditions in the aquifers of oil reservoirs (or active hydrodynamic conditions) is another reason for the occurrence of ROZs below the fluid contact. This happens when the aquifer formation crops out at the surface, where water can gain access and consequently changes the discharge pressure (Figure 8B). This results in a tilted present-day OWC, dipping in the downstream direction (Melzer et al., 2006). The degree of fluid contact tilt is controlled by

349 the rate of water movement in the aquifer, and the density difference between the oil and the
350 water. An increase in the hydrodynamic forces results in forced imbibition, and replacement
351 of the oil by water (Figure 8B). As forced imbibition leads to negative capillary pressure, the
352 residual oil saturation in this type of ROZ is lower than in the other two types of ROZ
353 (breached seal and tectonic tilt).

354 Although tilted OWCs resulting from hydrodynamic flow have been reported in a few fields
355 in the Middle East (Pelissier et al., 1980), evidence for this was not observed in any of the
356 studied fields. All of the studied fields show relatively horizontal present-day fluid contacts
357 (see fluid contact determination and Figure 3).

358 Also, in the Persian Gulf, the angle of tilt due to possible hydrodynamic activity is towards
359 the west/NW (Pelissier et al., 1980). If aquifer drive caused the ROZs, they would be seen in
360 the eastern and SE parts of the studied fields, and not in the northern parts. Furthermore, no
361 meaningful salinity variation in the aquifer (below FWL and OWC) has been observed, from
362 north to south or east to west in each field. Therefore, it is unlikely that hydrodynamic aquifer
363 generated the ROZs below the fluid contacts in the studied fields.

364 **Regional or local basin tilt.** ROZs below fluid contacts can be generated by regional
365 tectonic tilting and oil remobilisation (Figure 8C). Residual oil is left behind because of the
366 buoyancy of oil. Oil is displaced by the spontaneous imbibition of formation waters into the
367 reservoir as the oil evacuates upwards. These reservoirs with ROZ normally constitute
368 significant intervals of residual oil if the size of the field and/or basin tilting is considerable
369 (Melzer et al., 2006). Fields with ROZs below the fluid contact because of tectonic tilting
370 show flat present-day fluid contacts (Figure 8C). They also show ROZs below the fluid
371 contact and towards the down-dip direction (Figure 8C). This tilting process of ROZ

372 generation below the present-day FWL and OWC towards the NE matches the pattern of
373 geological events in the Persian Gulf towards the Zagros.

374 Consequently, it was concluded that the additional flexural loading and north to NE
375 downwards tectonic tilting after the Miocene (Figure 6) could explain the presence of the
376 ROZ below the present day FWL and OWC in the studied fields in the Persian Gulf better
377 than the other processes described.

378 The presence of residual oil below the present-day fluid contacts is due to a change in the
379 fluid contact position caused by tectonic basin tilting, and consequent structural tilting,
380 millions of years after the generation of the oil and its migration into the reservoirs. This
381 structural tilting has played a consequential role in the equilibrium of the reservoirs and their
382 fluid contents. Following this, the hydrocarbons and water attempted to achieve a new
383 equilibrium. Under these conditions, early migrated and accumulated oil was flushed out by
384 water (imbibition), and a ROZ was left below the present-day FWL and OWCs.

385 Figure 9A shows N/NE to S/SW cross-sections through Field A, before and after the Middle
386 Miocene. Five different areas (1–5) are defined. As oil was generated in the source rock at
387 around 39 Ma, and then migrated into the reservoir formation some 26 Ma (at the beginning
388 of the Lower Fars deposition), it is suggested that the reservoir structure was filled with oil
389 from the crest downwards, with the final stage represented by the palaeo-OWC. Therefore,
390 Regions 1 and 5 were located below the fluid contact, and Regions 2, 3 and 4 were above the
391 contact, after the time of oil filling. At this time, the oil saturation profile above the fluid
392 contact is represented by drainage capillary pressure curves (Adams, 2016).

393 From the Middle Miocene to the present, additional flexural loading and north to NE
394 downwards tectonic tilting caused the intervals located in Regions 2 and 4 to move below the

depths of the FWL and OWC (Figure 9B). Water once again penetrated the pore spaces in parts of Regions 2 and 4, and some (but not all) of the early accumulated oil was displaced by water. Subsequent to this fluid movement, residual oil was established below the new FWL and OWC depths in Regions 2 and 4, not only because the water was no longer the only wetting phase (McPhee et al., 2015), but also because not all of the oil was flushed out, with a percentage of it being trapped in some of the pores. The hydrocarbon saturation profile at this stage is represented by imbibition capillary pressure curves (Adams, 2016).

Based on the suggested model, all of the reservoirs filled by migrated oil before the Miocene should present both palaeo and present-day fluid contacts in the northern wells drilled beyond the present-day reservoir boundary. There is a delineation well that was drilled on the northern flank of Field A (A4) and penetrates reservoir formation beyond the determined FWL and OWC. This well presents a palaeo-OWC that is 42 m deeper than the present-day FWL and OWC.

As mentioned in fluid contact determination, Field A exhibits a FWL at 2900 m TVDSS in Well A6, drilled in the northern part of this field. This FWL is confirmed by the same OWC depth, determined in other wells. The A6 appraisal well was drilled to locate the FWL and OWC in the northern part of the field, and to determine the thickness of the reservoir and assess the characteristics and the productivity of the reservoir. Well A6 has petrophysical logs, mud-logging gas data, core data, formation pressure data and DSTs. Analysis of these data, particularly the formation pressure data, leads to a FWL at 2900 m TVDSS (Figures 2A and 10). In the same well, the results of the petrophysical evaluation indicated a significant percentage of residual oil below 2900 m TVDSS (Figure 10, track 8), where the residual oil saturation (ROS) was computed to be in the range of 50%. In addition, the core data shows oil-staining below 2900 m TVDSS (Figure 10, track 10).

Well A4 was drilled 3000 m from Well A6 to locate the northern limit of Field A (Figure 9). This well has a set of data that includes petrophysical logs, a DST, mud-logging gas chromatography and core data. The top of the Sarvak (Mishrif) reservoir is seen at 2912 m TVDSS in Well A4 (Figure 11), which is 12 m below the FWL determined by pressure data in nearby Well A6 (Figures 2A and 10). In Well A4, the upper part of the Sarvak (Mishrif) Fm does not correspond to 100% Sw, as would be expected below the FWL, but only to 70%, which equates to a 30% oil saturation (Figure 11, tracks 7, 8). The available DST data (2922 to 2965 m TVDSS) shows that this oil is residual oil that has been left behind, and is not movable. The presence of residual oil was also confirmed by core oil-staining. At the bottom of the ROZ, the Sw increases to 100% on the CPI (Figure 11), without any oil-staining or fluorescence on the cores, suggesting the presence of a palaeo-OWC at 2942 m TVDSS (42 m deeper than the present-day FWL and OWC). This is the position of the fluid contact of Field A in the Sarvak (Mishrif) Fm, before northwards tilting from the extra loading and forebulge movement towards the Zagros that occurred after the Middle Miocene.

The flexural loading is clear on N–S regional seismic lines from the Persian Gulf. Figure 12A shows a 140-km-long seismic line, near to Field C. This seismic line shows the asymmetric and wedge-shaped Persian Gulf. Major variations in sediment thicknesses, from south to north, began after the Middle Miocene. The Middle Miocene horizon shows a 2050 m flexural load over 140 km, suggesting a tilt of 0.836° for the Persian Gulf foreland basin. Figure 12B shows a NE–SW acoustic impedance section through Field B that emphasises a similar northward tilting.

Where no proper seismic section was available (e.g. Field A), a comparison of formation thickness and structural growth was used to explore the effect of tilting on formation thickness and sedimentation. Several cross-sections, each based on three wells, were prepared

443 across the field. Variations in formation thickness were calculated by subtracting the
444 formation thickness in the crestal well (A2) from those in the flank wells (A4, A5, A6, A38).
445 Figure 13 shows the results from Field A, illustrating how formation thicknesses vary across
446 the field through time, relative to those at the crest of the structure.

447 Figure 13 A and B show that structuration was effective at the end of Mishrif deposition.
448 Thicker deposits of up to 80m of Sarvak (Mishriff) Fm accumulated around the flanks of the
449 structure and is very clear on plots.

450 By the time of deposition of the Pabdeh Fm in the Eocene, a change in depositional patterns
451 had occurred. In the northern and north eastern wells of field (A4, A5 and A6), thinner
452 deposits are observed compared to the southern well, A38. This indicates less
453 accommodation space to the north and east of the structure during this time and a greater
454 sediment supply from the south.

455 Both cross sections illustrate an increase in the thickness of the formations deposited since
456 the Miocene (Guri, Gachsaran, Mishan, Aghajari and Bakhtiyari Fms) in the northern wells
457 (A4 and A6) compared to the central (A2) and southern wells (A5 and A38). This suggests
458 that more accommodation space began to be generated to the north of Field A after the
459 Middle Miocene. More accommodation space was provided by additional tilting towards the
460 north and NW, which was superimposed on the entire basin.

461 ## 7. Conclusions

462 The results of extensive regional studies were integrated with the data from three selected
463 fields in the Persian Gulf to present a geological model that would explain the presence of
464 residual oil below the present-day FWL and OWC in the area.

465 It was concluded that the presence of residual oil below the present-day FWL and OWC is
466 related to the geotectonic and plate margin evolution of the region, particularly the
467 convergence and collision of the Afro–Arabian and Eurasian Plates. In these fields, the
468 residual oil below the present-day FWL and OWC can be best explained by a change in the
469 fluid contact position caused by extra flexural loading and northwards tectonic tilting that
470 occurred millions of years after the generation and migration of the oil into the structures.

471 From the Late Turonian, the crustal thickening associated with the tectonic evolution caused
472 the lithosphere to bend, resulting in the development of a foreland basin and its forebulge to
473 the south and SW of the Zagros. The Zagros foreland basin includes the terrestrial
474 Mesapotamia and Persian Gulf Basins.

475 The crustal thickening associated with the tectonic evolution in the area creating the Zagros
476 provided a huge sediment supply to the foreland basin. As a result of this massive sediment
477 supply, and the increasing burial of older formations, the source rocks entered the oil window
478 around the Eocene. The generated oil migrated into the reservoirs through faults and fractures
479 before the Miocene.

480 From the Miocene onwards, reverse faulting and overfolding developed across the Zagros,
481 extending to the foreland basin, and leading to extra faulting, folding and migration of the
482 Zagros Orogeny towards its foreland basin (Persian Gulf).

483 The Zagros Mountains developed their present configuration before the end of the Neogene.
484 In response to this additional huge loading on the continental margin, the forebulge amplitude
485 increased, and its location moved towards the uplifted Zagros, and consequently the Persian
486 Gulf became narrower. This exerted a north to NE downward tilting on the entire basin,

including all structures and reservoirs filled by hydrocarbons, from the crest to the fluid contact or spill point.

Tectonic tilting changed the position of the fluid contacts in these fields, and therefore the equilibrium of the reservoir fluid contents. Following this, the hydrocarbons and water attempted to achieve a new equilibrium. Water once again penetrated the pore space in parts of the reservoirs (located above the older contact, but below the new fluid contact), and early accumulated oil was displaced by water. Subsequent to this fluid movement, residual oil was established below the new contact, not only because the water was no longer the only wetting phase, but also because not all of the oil was flushed out, a percentage of it being trapped. The hydrocarbon saturation profile at this stage is represented by imbibition capillary pressure curves.

The tilting angle of the foreland basin (Persian Gulf) was calculated to be around 0.836°.

Acknowledgments

The authors would like to acknowledge, and gratefully appreciate the support of, the Aberdeen Formation Evaluation Society for their sponsorship, and Emerson (Paradigm) for providing the Geolog software for the development of this study.

References

Abdollahie Fard, I., Sepehr, M., Sherkati, S., 2011. Neogene salt in SW Iran and its interaction with Zagros folding. Geological Magazine 148, 854-867.

Adams, S., 2016. Saturation-Height Modelling for Reservoir Description. The Petrophysicist Limited. ISBN: 9780473355197.

508 Agard, P., Omrani, J., Jolivet, L., Mouthereau, F., 2005. Convergence history across Zagros
509 (Iran): Constraints from collisional and earlier deformation. International Journal of Earth
510 Sciences (Geologische Rundschau) 94, 401-419.

511 Agard, P., Omrani, J., Jolivet, L., Whitechurch, H., Vriielynck, B., Sparkman, W., Monie, P.,
512 Meyer, B., Wortel, R., 2011. Zagros orogeny: A subduction-dominated process. Geological
513 Magazine 148, 692-725.

514 Ala, M. A., 1982. Chronology of trap formation and migration of hydrocarbons in the Zagros
515 sector of southwest Iran. AAPG Bulletin 66, 1535-1541.

516 Ala, M. A., Kinghorn, R. R. F., Rahman, M., 1980. Organic geochemistry and source rock
517 characteristics of the Zagros petroleum province, southwest Iran. Journal of Petroleum
518 Geology 3, 61-89.

519 Alavi, M., 1980. Tectonostratigraphic evolution of the Zagrosides of Iran. Geology 8, 144-
520 149.

521 Alavi, M., 1994. Tectonics of the Zagros orogenic belt of Iran: New data and interpretations.
522 Tectonophysics 229, 211-238.

523 Alavi, M., 1996. Tectonostratigraphic synthesis and structural style of the Alborz mountain
524 system in northern Iran. Journal of Geodynamics 21, 1-33.

525 Alavi, M., 2004. Regional stratigraphy of the Zagros fold thrust belt of Iran and its
526 proforeland evolution. American Journal of Science 304, 1-20.

527 Alavi, M., Mahdavi, M. A., 1994. Stratigraphy and structures of the Nahavand region in
528 western Iran and their implications for the Zagros tectonics. Geological Magazine 131, 43-47.

529 Aleidan, A., Kwak, H., Muller, H., Zhou, X., 2017. Residual-Oil Zone: Paleo-Oil
530 Characterization and Fundamental Analysis. Society of Petroleum Engineers, 260-268.

531 Ali, M., Watts, A. B., 2009. Subsidence history, gravity anomalies and flexure of the United
532 Arab Emirates (UAE) foreland basin. GeoArabia 14(2), 17-44.

533 Allen, M., Talebian, M., 2011. Structural variation along the Zagros and the nature of the
534 Dezful Embayment. Geological Magazine 148(5–6), 911-924.
535 doi:10.1017/S0016756811000318

536 Alsharhan, A. S., Nairn, A. E. M., 1997. Sedimentary Basins and Petroleum Geology of the
537 Middle East. Elsevier Science Publishing: Netherlands.

538 Arian, M., Noroozpoor, H., 2015. Tectonic Geomorphology of Iran's Salt Structures. Open
539 Journal of Geology 5, 61-72.

540 Arrajehi, A., Mcclusky, S., Reilinger, R., Daoud, M., Alchalbi, A., Ergintav, S., Gomez, F.,
541 Sholan, J., Bou-Rabee, F., Ogubazghi, G., Haileab, B., Fisseha, S., Asfaw, L., Mahmoud, S.,
542 Rayan, A., Bendik, R., Kogan, L., 2010. Geodetic constraints on the present-day motion of
543 the Arabian Plate: Implications for Red Sea and Gulf of Aden rifting. Tectonics 29,
544 https://doi.org/10.1029/2009TC002482.

545 Bahroudi, A., Koyi, H. A., 2003. Effect of the spatial distribution of Hormuz salt on
546 deformation style in the Zagros fold and thrust belt: An analogue modelling approach.
547 Journal of the Geological Society, London 160, 719-733.

548 Bahroudi, A. and Koyi, H. A., 2004. Tectono-sedimentary framework of the Gachsaran
549 Formation in the Zagros foreland basin. Marine and Petroleum Geology 21, 1295-1310.

550 Berberian, F., Muir, I. D., Pankhurst, R. J., Berberian, M., 1982. Late Cretaceous and early
551 Miocene Andean type plutonic activity in northern Makran and Central Iran. Journal of
552 Geological Society, London 139, 605-614.

553 Berberian, M., King, G. C. P., 1981. Towards a paleogeography and tectonic evolution of
554 Iran. Canadian Journal of Earth Sciences 18, 1764-1766.

555 Beydoun, Z. R., Hughes, M. W., Stoneley, R., 1992. Petroleum in the Zagros basin: A late
556 Tertiary foreland basin overprinted onto the outer edge of the vast hydrocarbon-rich
557 Paleozoic-Mesozoic passive margin shelf. AAPG Memoir 55, 307-336.

558 Bordenave, M. L., 2002. Gas prospective areas in the Zagros domain of Iran and the gulf
559 Iranian waters. AAPG Annual meeting, March 10-13, Houston, Texas.

560 Carpentier, B., Arab, H., Pluchery, E., Chautrau, J., 2006. Tar mats and residual oil
561 distribution in a giant oil field offshore Abu Dhabi. Journal of Petroleum Science and
562 Engineering 58, 472-490.

563 Chung, S. L., Zarrinkoub, M. H., Karakhanyan, A. S., Javakhishvili, Z.,Lo, C. H., 2010. A
564 comparative study of the Tibet/Himalaya and Caucasus/Iran orogenic belts: Magmatic per-
565 spectives, tectonic crossroads: Evolving orogens of Eurasia-Africa-Arabia. GSA: Ankara,
566 Turkey.

567 Colman-Sadd, S., 1978. Fold development in the Zagros simply folded belt, Southwest Iran.
568 AAPG Bulletin 62, 984-1003.

569 Darling, T., 2005. Well Logging and Formation Evaluation. Gulf Professional Publishing:
570 ISBN 9780750678834

571 Decelles, P. G., Giles, K. A., 1996. Foreland basin systems. Basin Research 8, 105-123.

572 Dercourt, J., Ricou, L. E., Vrielynck, B., 1993. Atlas of Tethys Palaeoenvironmental maps.
573 Gauthier-Villars: Paris

574 Dercourt, J., Zonenshain, L. P., Ricou, L.-E., Kazmin, V. G., Le pichon, X., Knipper, A. L.,
575 Grandjacquet, C., Sbortshikov, I. M., Geyssant, J., Lepvrier, C., Pechersky, D. H., Boulin, J.,
576 Sibuet, J.-C., Savostin, L. A., Sorokhtin, O., Westphal, M., Bazhenov, M. L., Lauer, J. P.,
577 Biju-Duval, B., 1986. Geological evolution of the Tethys belt from the Atlantic to the Pamirs
578 since the Lias. Tectonophysics 123, 241-315.

579 Dickson, W. R., 1974. Plate tectonics and sedimentation. Special Publication of the SEPM
580 22, 1-27. doi:10.1029/2005JB003791

581 Elshahawi, H., Fathy, K., Hiekal, S., 1999. Capillary Pressure and Rock Wettability Effects
582 on Wireline Formation Tester Measurements. Society of Petroleum Engineers.
583 doi:10.2118/56712-MS

584 Emami, H., 2008. Foreland propagation of folding and structure of the Mountain Front
585 Flexure in the Pusht-e Kuh Arc (NW Zagros, Iran). PhD thesis, University of Barcelona, pp.
586 1-181.

587 Emery, K. O., 1956. Sediments and water of the Persian Gulf. Bulletin of the AAPG 40,
588 2354-2383.

589 Faghih, A., Sarkarinejad, K., 2011, Kinematics of rock flow and fabric development
590 associated with shear deformation within the Zagros transpression zone, Iran. Geological
591 Magazine 148, 1009-1017.

592 Falcon, N. L., 1969. Problems of the relationship between surface structure and deep
593 displacements illustrated by the Zagros range. Geological Society of London, Special
594 Publication 5, 9-22.

595 Falcon, N. L., 1974. An outline of the geology of the Iranian Makran. Geographical Journal
596 140, 283-291.

597 Falcon, N. L., 1974. Southern Iran: Zagros Mountains. Geological Society of London,
598 Special Publication 4, 199-211.

599 Farzadi, P., 2006. The development of Middle Cretaceous carbonate platforms, Persian Gulf,
600 Iran: Constraints from seismic stratigraphy, wells and biostratigraphy. Petroleum Geoscience
601 12, 59-68.

602 Farzipour-Saein, A., Yassaghi, A., Sherkati, S., Koyi, H., 2009. Basin evolution of the
603 Lurestan Region in the Zagros Fold-and-Thrust Belt, Iran. Journal of Petroleum Geology
604 32(1), 5-20.

605 Ghasemi-Nejad, E., Head, M., Naderi, M., 2009. Palynology and petroleum potential of the
606 Khazhdumi Formation (Cretaceous: Albian-Cenomanian) in the South Pars field, northern
607 Persian Gulf. Marine and Petroleum Geology 26, 805-816.

608 Ghazban, F., Motiei, H., 2010. Petroleum Geology of the Persian Gulf, Iran. National Iranian
609 Oil Company Publications, ISBN 9789640394205

610 Hafkenscheid, E., Wortel, M. J. R., Spakman, W., 2006. Subduction history of the Tethyan-
611 derived seismic tomography and tectonic reconstruction. Journal of Geophysical Research
612 111, B08401.

613 Harouaka, A., Trentham, B., Melzer, S., 2013. Long Overlooked Residual Oil Zones (ROZs)
614 Are Brought into the Limelight. Society of Petroleum Engineers, 167209.

615 Homke, S., Verges, J., Garces, M., Emami, H., Karpuz, R., 2004. Magnetostratigraphy of
616 Miocene–Pliocene Zagros foreland deposits in the front of the Push-e Kush Arc (Lurestan
617 Province, Iran). Earth and Planetary Science Letters 225(3-4), 397-410.

618 Homke, S., Vergés, J., Serra-Kiel, J., Bernaola, G., Sharp, I., Garcés, M., Montero-Verdù, I.,
619 Karpuz, R., Goodarzi, M. H., 2009. Late Cretaceous-Paleocene formation of the proto-Zagros
620 foreland basin, Lurestan Province, SW Iran. GSA Bulletin 121, 963-978.

621 Hooper, R. J., Baron, I. R., Agah, S., Hatcher, R. D., 1994. The Cenomanian to Recent
622 development of the southern Tethyan Margin in Iran. In: Al-Husseini, M. I. (ed.), Middle
623 East Petroleum Geosciences, GEO 94(2), pp. 505-516. Gulf PetroLink: Bahrain.

624 Jahani, S., Callot, J.-P., Letouzey, J., Frizon de Lamotte, D., 2009. The eastern termination of
625 the Zagros Fold-and-Thrust Belt, Iran: Structures, evolution, and relationships between salt
626 plugs, folding, and faulting. Tectonics 28, TC6004. doi:10.1029/2008TC002418

627 James, G. A., Wynd, J. G., 1965. Stratigraphical nomenclature of Iranian Oil Consortium
628 agreement area. AAPG Bulletin 49, 2182-2245.

629 Jolivet, L., Faccenna, C., 2000. Mediterranean extension and the Africa-Eurasia collision.
630 Tectonics 19, 1095-1106.

631 Jordan, C.F., Connally, T.C., Vest, H.A., 1985. Middle Cretaceous carbonates of the Mishrif
632 Formation, Fateh Field, Offshore Dubai, U.A.E. In: Roehl, P. O., Coquette, P. W. (eds),
633 Carbonate Petroleum Reservoirs, pp. 425-442. Springer-Verlag: New York.

634 Kent, P. E., 1979. The emergent Hormuz salt plugs of southern Iran. Journal of Petroleum
635 Geology 2, 117-144.

636 Khadivi, S., Mouthereau, F., Barbarand, J., Adatte, T., Lacombe, O., 2012. Constraints on
637 paleodrainage evolution induced by uplift and exhumation on the southern flank of the
638 Zagros-Iranian Plateau. Journal of the Geological Society of London 169, 83-97.

639 Kirkham, A., Bin Joma, M., Mckean, T. A. M., Palmer, A. F., Smith, M. J., Thomas, H.,
640 Twombley, B., 1996. Fluid saturation prediction in a transition zone. GeoArabia 1(4), 551-
641 566.

642 Koop, W., Stoneley, R., 1982. Subsidence history of the Middle East Zagros basin, Permian
643 to Recent. Philosophical Transactions of the Royal Society of London 305, 149-168.

644 Koperna, G. J., Melzer, L. S., Kuuskraa, V. A., 2006. Recovery of oil resources from the
645 residual and transitional oil zones of the Permian Basin. Society of Petroleum Engineers,
646 102972.

647 Lacombe, O., Bellahsen, N., Mouthereau, F., 2011. Fracture patterns in the Zagros Simply
648 Folded Belt (Fars, Iran): Constraints on early collisional tectonic history and role of basement
649 faults. Geological Magazine 148, 940–963. doi:10.1017/S001675681100029X

650 Lacombe, O., Mouthereau, F., Kargar, S., Meyer, B., 2006. Late Cenozoic and modern stress
651 fields in the western Fars (Iran): Implications for the tectonic and kinematic evolution of
652 central Zagros. Tectonics 25, TC1003. doi:10.1029/2005TC001831

653 Leroy, S., Gente, P., Fournier, M., D'acremont, E., Patriat, P., Beslier, M. O., Bellahsen, N.,
654 Maia, M., Blais, A., Perrot, J., Al-Kathiri, A., Merkouriev, S., Fleury, J. M., Ruellan, P. Y.,
655 Lepvrier, C., Huchon, P., 2004. From rifting to spreading in the eastern Gulf of Aden: A

656 geophysical survey of a young oceanic basin from margin to margin. Terra Nova 16(4), 185-
657 192.

658 Mcphee, C., Reed, J., Zubizarreta, I., 2015. Core Analysis: A Best Practice Guide.
659 Developments in Petroleum Science 64.

660 Mcquarrie, N., 2004. Crustal scale geometry of the Zagros fold-thrust belt, Iran. Journal of
661 Structural Geology 26, 519-535.

662 Mcquarrie, N., Stock, J. M., Verdel, C., Wernicke, B. P., 2003. Cenozoic evolution of
663 Neotethys and implications for the causes of plate motions. Geophysical Research Letters 30.
664 doi:10.1029/2003GL017992

665 Melzer, L. S., Kuuskraa, V. A., Koperna, G. J., 2006. The Origin and Resource Potential of
666 Residual Oil Zones. Society of Petroleum Engineers, 102964.

667 Miall, A., 2010. Principles of Sedimentary Basin Analysis. Springer-Verlag, New York.

668 Mina, P., Razaghnia, M. T., Paran, Y., 1967. Geological and geophysical studies and
669 exploratory drilling of the Iranian continental shelf–Persian Gulf. Proceedings of the Seventh
670 World Petroleum Congress, Mexico 2, 771-903.

671 Mohajjel, M., Fergusson, C. L., 2000. Dextral transpression in Late Cretaceous continental
672 collision, Sanandaj-Sirjan Zone, western Iran. Journal of Structural Geology 22, 1125-1139.

673 Molinaro, M., Leturmy, P., Guezou, J. C., Frizon de Lamotte, D., Eshraghi, S. A., 2005. The
674 structure and kinematics of the south-eastern Zagros fold-thrust belt; Iran: From thin-skinned
675 to thick-skinned tectonics. Tectonics 24. 10.1029/2004TC001633.

676 Morris, P., 1977. Basement structure as suggested by aeromagnetic surveys in southwest Iran.
677 Internal report of National Iranian Oil Company.

678 Motiei, H., 1995. Petroleum Geology of Zagros. In: Hushmandzadeh, A. (ed.), Treatise on the
679 Geology of Iran. Geological Survey of Iran, Iran.

680 Mouthereau, F., 2011. Timing of uplift in the Zagros belt/Iranian plateau and accommodation
681 of late Cenozoic Arabia–Eurasia convergence. Geological Magazine 148, 726-738.

682 Mouthereau, F., Lacombe, O., Verges, J., 2012. Building the Zagros collisional orogen:
683 Timing, strain distribution and the dynamics of Arabia/Eurasia plate convergence.
684 Tectonophysics. s 532-535. 27-60. 10.1016/j.tecto.2012.01.022.

685 Mouthereau, F., Tensi, J., Bellahsen, N., Lacombe, O., De Boisgrollier, T., Kargar, S., 2007.
686 Tertiary sequence of deformation 26, TC5006. doi: 10.1029in a thin-skinned/thick-skinned
687 collision belt: The Zagros Folded Belt (Fars, Iran). Tectonics /2007TC002098

688 Murris, R. J., 1980. Middle East: Stratigraphic evolution and oil habitant. Geologie en
689 Mijnbouw 60, 467–486.

690 O'sullivan, T., Praveer, K., Shanley, K., Dolson, J. C., Woodhouse, R., 2010. Residual
691 hydrocarbons-a trap for the unwary. Society of Petroleum Engineers 128013.

692 Parker, A. R., Rudd, J. M., 2000. Understanding and Modelling Water Free Production In
693 Transition Zones. Society of Petroleul Engineers 59412.

694 Pelissier, J., Hedayati, A. A., Abgrall, E., Plique, J., 1980. Study of Hydrodynamic Activity
695 in the Mishrif Fields, Offshore Iran. Society of Petroleum Engineers. doi:10.2118/7508-PA.

696 Pirouz, M., Simpson, G., Bahroudi, A., Azhdari, A., 2011. Neogene sediments and modern
697 depositional environments of the Zagros foreland basin system. Geological Magazine 148,
698 838-853.

699 Purser, B., 1973. The Persian Gulf: Holocene carbonate sedimentation and diagenesis in a
700 shallow epicontinental sea. Springer-Verlag: Berlin and New York, pp. 157-177.

701 Robertson, A. H. F., 2000. Mesozoic–Tertiary tectonic sedimentary evolution of a south
702 Tethyan oceanic basin and its margins in southern Turkey. Geological Society of London,
703 Special Publication 173, 97-138.

704 Sengör, A. M. C., Altiner, D., Cin, A., Ustaömer, T., Hsü, K. J., 1988. The origin and
705 assembly of the Tethyside orogenic collage at the expense of Gondwanaland. Geological
706 Society of London, Special Publication 37, 119-181.

707 Sepehr, M., Cosgrove, J. W., 2004. Structural framework of the Zagros Fold-Thrust Belt,
708 Iran. Marine and Petroleum Geology 21, 829-843.

709 Setudehnia, A., 1978. The Mesozoic sequence in south-west Iran and adjacent areas. Journal
710 of Petroleum Geology 1, 3-42.

711 Sharland, P.R., Archer, R., Casey, D.M., Davies, R.B., Hall, S.H., Heward, A.P., Horbury,
712 A.D., Simmons, M.D., 2001. Arabian Plate Sequence Stratigraphy. Geo Arabia Special
713 Publication 2, Gulf PetroLink, Bahrain, 371 p.

714 Sherkati, S., Letouzey, J., 2004. Variation of structural style and basin evolution in the central
715 Zagros, Iran. Marine and Petroleum Geology 21(5), 535-554.

716 Sherkati, S., Letouzey, J., Frizon de Lamotte, D., 2006. Central Zagros fold-thrust belt (Iran):
717 New insights from seismic data, field observation and sandbox modelling. Tectonics 25,
718 TC4007. doi:10.1029/2004TC001766

719 Spinler, E. A., Baldwin, B. A., 1999. A direct method for determining complete positive and
720 negative capillary pressure curves for reservoir rock using the centrifuge. AAPG Memoir 71,
721 175-178.

722 Stampfli, G. M., Borel, G. D., 2002. A plate tectonic model for the Paleozoic and Mesozoic
723 constrained by dynamic plate boundaries and restored synthetic oceanic isochrons. Earth and
724 Planetary Science Letters 196, 17-33.

725 Stöcklin, J., 1968. Structural history and tectonics of Iran: A review. AAPG Bulletin 52,
726 1229-1258.

727 Stocklin, J., 1974. Possible ancient continental margins in Iran. In: Burk, C. A. and Drake, C.
728 L. (eds), The Geology of Continental Margins, pp. 873–887. Springer: Berlin.

729 Swift, S. A., Ross, D. A., 2002. Neogene Stratigraphic Development of the Persian Gulf,
730 Defence Technical Information Centre.

731 Szabo, F., Kheradpir, A., 1978. Permian and Triassic stratigraphy, Zagros Basin, south-west
732 Iran. Journal of Petroleum Geology 1, 57-82.

733 Tavani, S., Storti, F., Soleimany, B., Fallah, M., Munoz, J., Gambini, R., 2011. Geometry,
734 kinematics and fracture pattern of the Bangestan anticline, Zagros, SW Iran. Geological
735 Magazine 148, 964-979. 10.1017/S0016756811000197.

736 Thomasen, J. B., Jacobsen, N. L., 1994. Dipping Fluid Contacts in the Kraka Field, Danish
737 North Sea. Society of Petroleum Engineers. doi:10.2118/28435-MS.

738 Tiab, D., Donaldson, E. C., 2015. Petrophysics: Theory and practice of measuring reservoir
739 rock and fluid transport properties. Gulf Professional Publishing: Boston.

740 Uchupi, E., Swift, S. A., Ross D. A., 1999. Late Quaternary stratigraphy, paleoclimate and
741 neotectonism of the Persian (Arabian) Gulf region. Marine Geology 160, 1–2.

742 Vejbaek, O. V., Frykman, P., Nielsen, C. M., 2005. The history of the hydrocarbon filling of
743 Danish chalk fields. Geological Society of London 6, 1331-1345.

744 Verdel, C., Wernicke, B. P., Hassanzadeh, J, Guest, B., 2011. A Paleogene extensional arc
745 flare-up in Iran. Tectonics 30, TC3008.

746 Verges, J., Saura, E., Casciello, E., Fernàndez, M., Villasenor, A., Jimenez-Munt, I., Garcia-
747 Castellanos, D., 2011. Crustal-scale cross-sections across the NW Zagros belt: Implications
748 for the Arabian margin reconstruction. Geological Magazine. 10.1017/S0016756811000331

749 Vincent, S. J., Allen, M. B., Ismail-Zadeh, A. D., Flecker, R., Foland, K. A., Simmons, M.
750 D., 2005. Insights from the Talysh of Azerbaijan into the Paleogene evolution of the South
751 Caspian region. GSA Bulletin 117, 1513–1533.

752 Yilmaz, Y., 1993. New evidence and model on the evolution of the southeast Anatolian
753 orogen. GSA Bulletin 105, 251–271.

754 Ziegler, M. A., 2001. Late Permian to Holocene paleofacies evolution of the Arabian Plate
755 and its hydrocarbon occurrences. GeoArabia 6, 445–504.

756

757

758

Graphic Abstract: Presence of residual oil below the present-day FWL is related to the north-east downward tilting of the entire Persian Gulf foreland basin

Figure 1: Examples of the presence of residual oil below the FWL and OWC in three studied fields (A, B and C). Second track shows fliud content: green =oil, blue =water. More residual oil below the FWL and OWC is seen in the northerrn parts of each field.

Figure 2: Cross plots of static formation pressure data vs depth (TVDSS). A) FWL at 2900 m TVDSS in field A and B) FWL at 2337 m TVDSS in field C.

Figure 3: Fluid contact (blue line) determination in wells drilled and logged prior to the start of production in studied fields. Field A presents a FWL obtained from the formation pressure data in a northern well. This FWL is supported by the same OWC depth determined from the log data in two southern and one northern wells. A paleo OWC is seen at 2942 m TVDSS.

Field B shows an OWC at 1221 m TVDSS from the data of 5 wells located in different parts of the field. There is no formation pressure data in this field.

Field C illustrates a FWL at 2337 m TVDSS determined from the extrapolation of formation pressure data in a well located in the south of the field. Depth of this FWL is supported by ODT and WUT seen in a well drilled on the northern flank of the field.

Figure 4: Summary of regional geology in the area.

Figure 5: Sedimentation in the Persian Gulf foreland basin from the late Turonian to the Miocene. Location of field B on the basin is shown with rectangle.

Figure 6: Movement of the Persian Gulf forebulge toward the orogenic suture making the Persian Gulf narrower after Mid Miocene. Locations of field B before and after tectonic

subsidence is shown with dash and solid rectangles respectively. This exerted a northward tilting on the entire basin.

Figure 7: Sedimentation in the narrower and northwardly tilted Persian Gulf foreland basin from the Mid Miocene to the present. Location of field B on the basin (Sarvak Fm is the reservoir) is shown with rectangle.

Figure 8: The most important processes of forming ROZ prior to the start of reservoir production. A: leakage in the seal and cap rock, B: hydrodynamic and active aquifer, C: regional tilting.

Figure 9: Effect of basin tilting on FWL and OWC adjustment and and changing capillary pressure regimes across the field A,

A: Before Mid Miocene, regions 1 and 5 were located below the fluid contact and other areas (2, 3 and 4) were above the fluid contact.

B: After Mid Miocene, regions 1, 2, 4 and 5 were located below the fluid contact and area 3 were above the fluid contact. Early accumulated oil in regions 2 and 4 was displaced by water and residual oil was trapped below the new fluid contact.

Figure 10: Petrophysical evaluation of A6 showing a FWL at 2900 TVDSS. There is a thickness of residual oil zone and oil staining below this FWL.

Figure 11: Petrophysical evaluation of well A4. This well was drilled on the northern flank of field A beyond the FWL (2900 m TVDSS). Top Sarvak (Mishrif) is located 12 m below the present day FWL. 30% residual oil below the field FWL and OWC disappears at 2942 showing a paleo fluid contact.

Figure 12: A: Long regional seismic section (140 km) crossing field A illustrates asymmetric and wedge-shaped Persian Gulf foreland basin. The Mid Miocene horizon shows a 2050 m flexural load over 140 km suggesting a tilt of 0.836 degrees for the Persian Gulf foreland basin.

B: Acoustic Impedance section through Field B emphasises same northwardly tilting.

Figure 13: Thickness comparison and structural growth in one of the studied fields following deposition of the Sarvak (Mishriff) Fm reservoir. Both plots (A and B) show an increase in the thickness of formations deposited after the Miocene (Guri, Gachsaran, Mishan, Aghajari and Bakhtiyari Formations) in the northern wells (A4 and A6) compared to central (A2) and southern wells (A5 and A38). This is related to additional tilting toward N and NW which was superimposed to the entire basin after Mid Miocene.

- Residual oil occurs below the current fluid contact in many Middle Eastern reservoirs.
- This is related to tilting of the Arabian Plate towards the Zagros mountains.
- Tilting changed the equilibrium of the reservoirs and their fluid contents.
- Water partly replaced oil at the base of reservoirs creating residual oil zones.

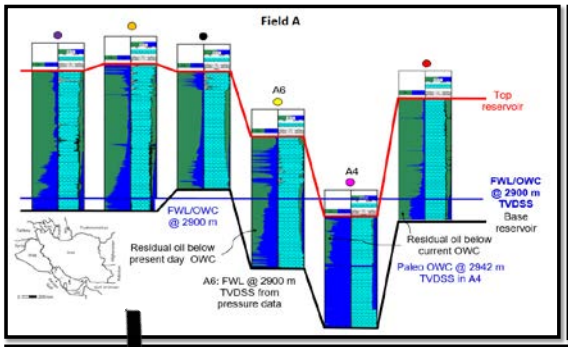

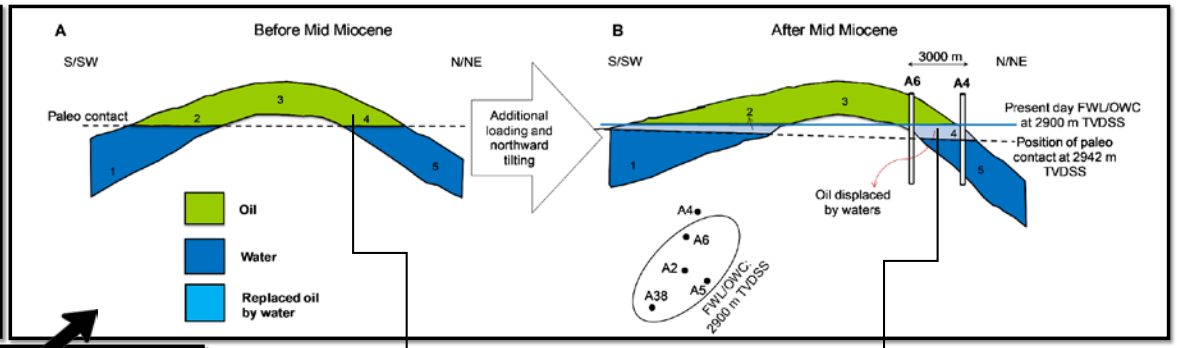

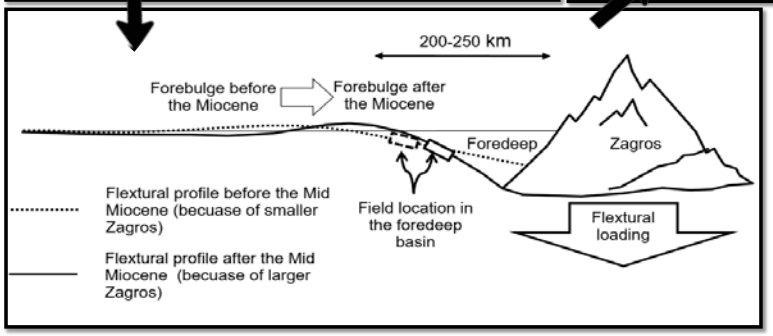

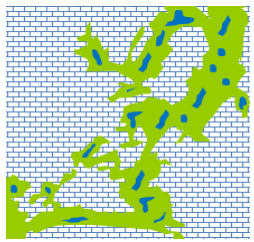

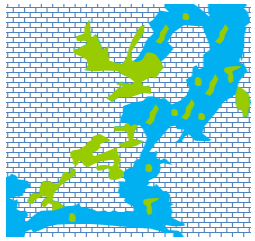

Residual oil after north-east downward tilting of the basin

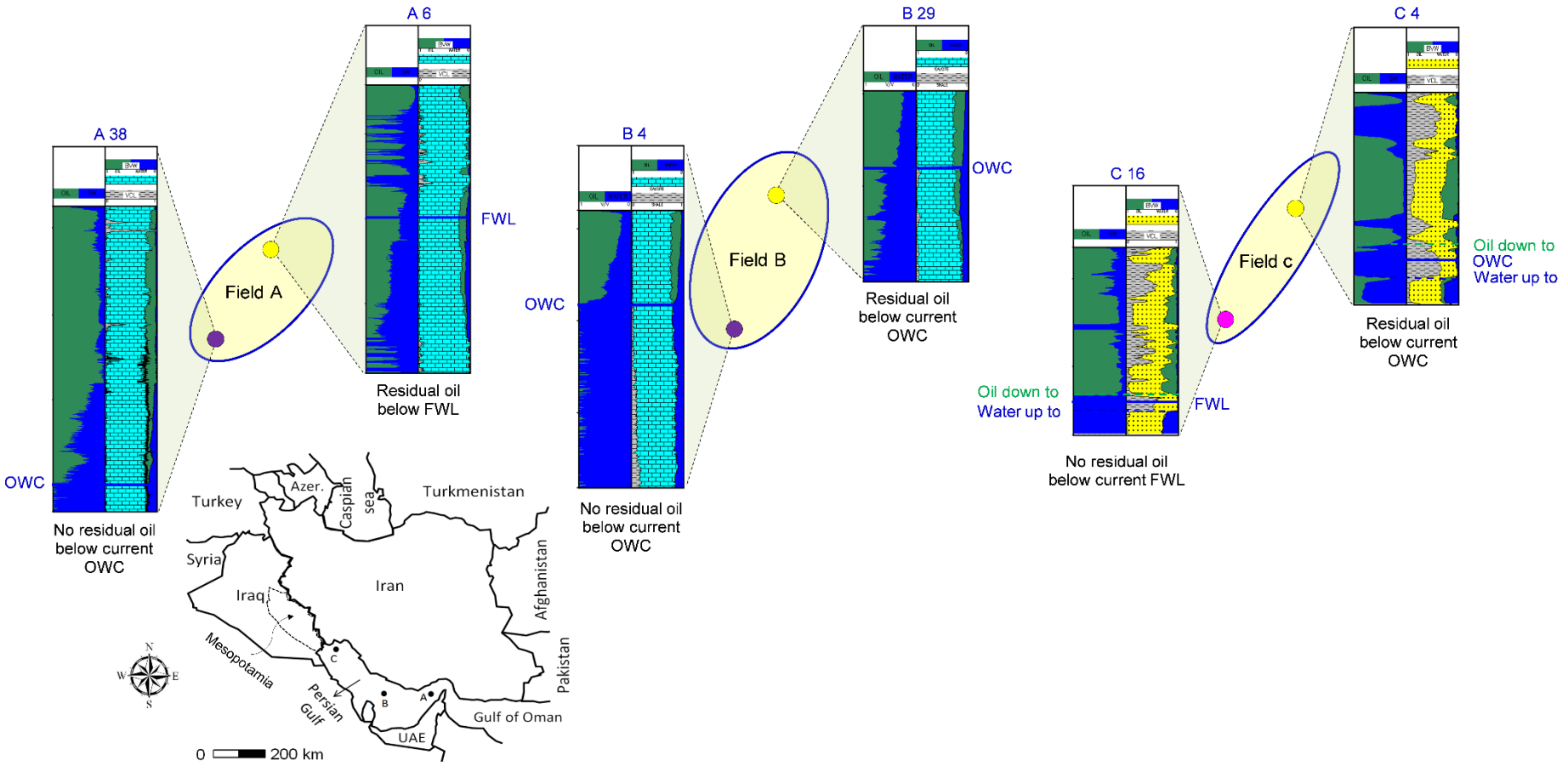

Figure 1: Examples of the presence of residual oil below the FWL and OWC in three studied fields (A, B and C). Second track shows fliud content: green =oil, blue =water. More residual oil below the FWL and OWC is seen in the northerrn parts of each field.

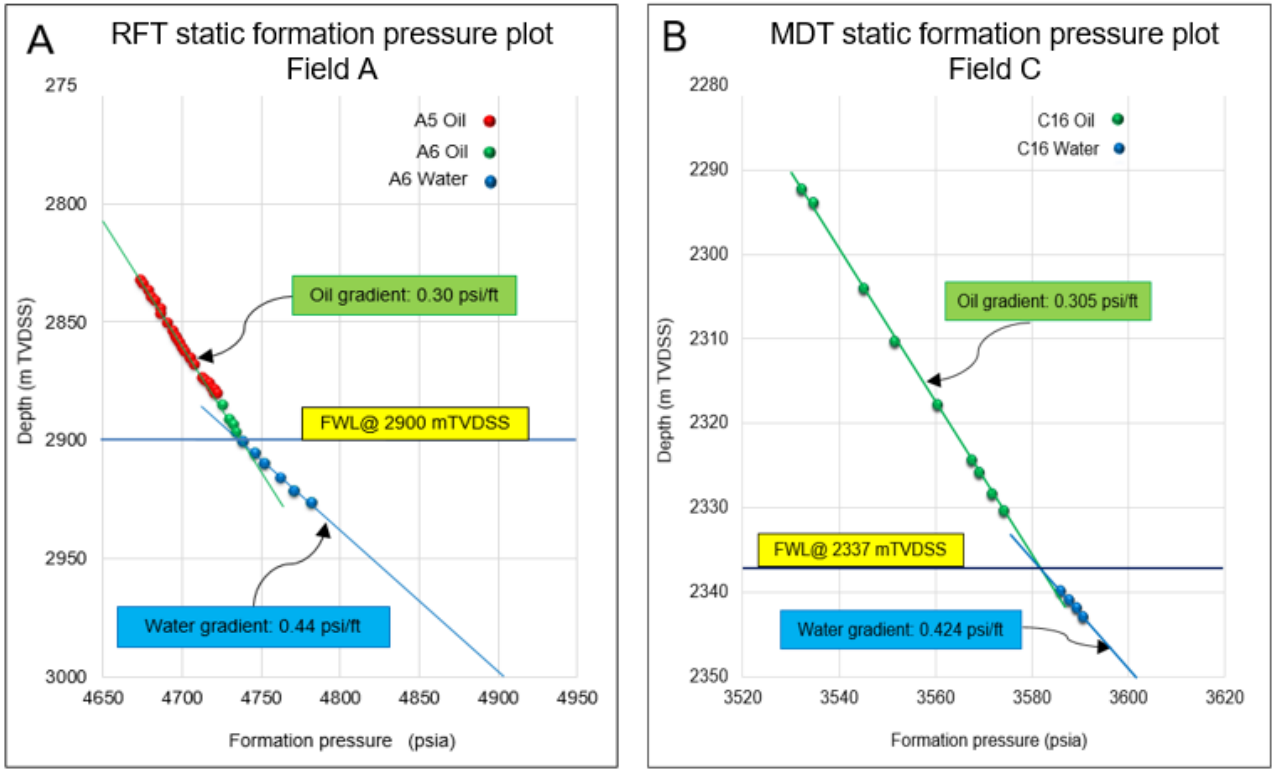

Figure 2: Cross plots of static formation pressure data vs depth (TVDSS). A) FWL at 2900 m TVDSS in field A and B) FWL at 2337 m TVDSS in field C.

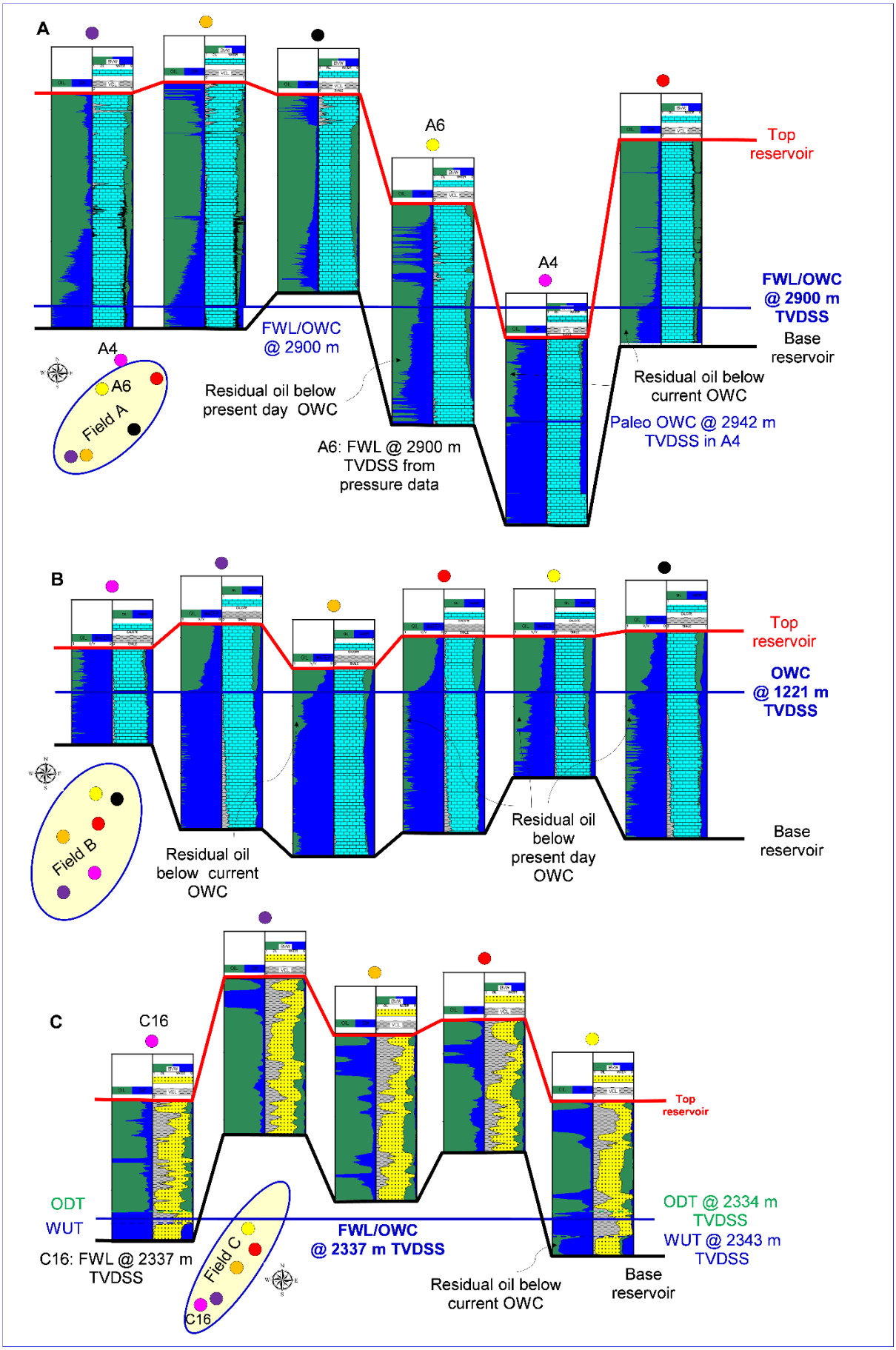
A
A6
Top reservoir
A4
FWL/OWC @ 2900 m TVDSS
Base reservoir
FWL/OWC @ 2900 m
A4
A6
Field A
Residual oil below present day OWC
Residual oil below current OWC
Paleo OWC @ 2942 m TVDSS in A4
A6: FWL @ 2900 m TVDSS from pressure data
B
Top reservoir
OWC @ 1221 m TVDSS
Base reservoir
Field B
Residual oil below current OWC
Residual oil below present day OWC
C
C16
Top reservoir
ODT
WUT
ODT @ 2334 m TVDSS
WUT @ 2343 m TVDSS
C16: FWL @ 2337 m TVDSS
Field C
FWL/OWC @ 2337 m TVDSS
Residual oil below current OWC
Base reservoir
C16

Figure 3: Fluid contact (blue line) determination in wells drilled and logged prior to the start of production in studied fields. Field A presents a FWL obtained from the formation pressure data in a northern well. This FWL is supported by the same OWC depth determined from the log data in two southern and one northern wells. A paleo OWC is seen at 2942 m TVDSS.

Field B shows an OWC at 1221 m TVDSS from the data of 5 wells located in different parts of the field. There is no formation pressure data in this field.

Field C illustrates a FWL at 2337 m TVDSS determined from the extrapolation of formation pressure data in a well located in the south of the field. Depth of this FWL is supported by ODT and WUT seen in a well drilled on the northern flank of the field.

<table>
<tr><th>Era</th><th>System / Period</th><th>Series</th><th>Ocean</th><th>Continents</th><th>Setting</th><th>Geological Event</th><th>Tectono-stratigraphy</th><th>Field</th></tr>
<tr><td rowspan="5">Cenozoic</td><td colspan="2">Quaternary</td><td></td><td rowspan="15"></td><td rowspan="5">Arabian - Eurasia collision
Africa-Arabia separation</td><td rowspan="5">Active Margin</td><td rowspan="2">Maximum collision in the Zagros, faulting and folding, Forebulge movement</td><td rowspan="5"></td><td rowspan="2">Large tilting in foreland basin</td></tr>
<tr><td rowspan="4">Tertiary</td><td rowspan="2">Neogene</td><td rowspan="2">Pliocene - Oligocene</td></tr>
<tr><td rowspan="3">Uplift

Magmatism</td><td rowspan="3">Proforeland basin</td><td rowspan="2">Oil migration

Oil generation</td></tr>
<tr><td rowspan="2">Paleogene</td><td rowspan="2">Paleocene - Eocene</td></tr>
<tr><td rowspan="10">Mesozoic</td><td colspan="2" rowspan="3">Cretaceous</td><td>Upper</td><td rowspan="4">Arabian and Eurasia converge</td><td rowspan="4">Subduction, Ophiolite obduction and Initiation of Foreland basin</td><td rowspan="2">Rising of structures due to salt diapirism</td></tr>
<tr><td rowspan="2">Lower</td><td rowspan="2">Neo-Tethys</td></tr>
<tr><td rowspan="5">Passive Margin</td><td rowspan="2">Break away of India</td></tr>
<tr><td colspan="2" rowspan="4">Jurassic</td><td>Malm</td><td rowspan="2">Neo-Tethyan continental shelf</td></tr>
<tr><td rowspan="2">Dogger</td><td rowspan="3">Gondwana</td></tr>
<tr><td>Liassic</td><td>Collision of Sanandaj-Sirjan to Eurasia</td></tr>
<tr><td colspan="2">Triassic</td><td></td><td rowspan="2">Pangea</td><td>Rifting and forming of Neo Tethys</td><td rowspan="2">Epi-Pangean platform</td></tr>
<tr><td rowspan="5">Paleozoic</td><td colspan="2">Permian</td><td rowspan="2">Paleo-Tethys</td><td rowspan="4">Intra-Craton</td></tr>
<tr><td colspan="2">Dev.-Carbon.</td><td></td></tr>
<tr><td colspan="2">Silurian</td><td></td><td rowspan="3">Najd Rift</td><td rowspan="3">Pull-apart and epicontinental platform basins</td></tr>
<tr><td colspan="2">Ordovician</td><td></td></tr>
<tr><td colspan="2">Cambrian</td><td>Proto-Tethys</td></tr>
<tr><td>Prec.</td><td colspan="2"></td><td></td><td></td><td></td><td></td><td></td><td></td></tr>
</table>

Figure 4: Summary of regional geology in the area.

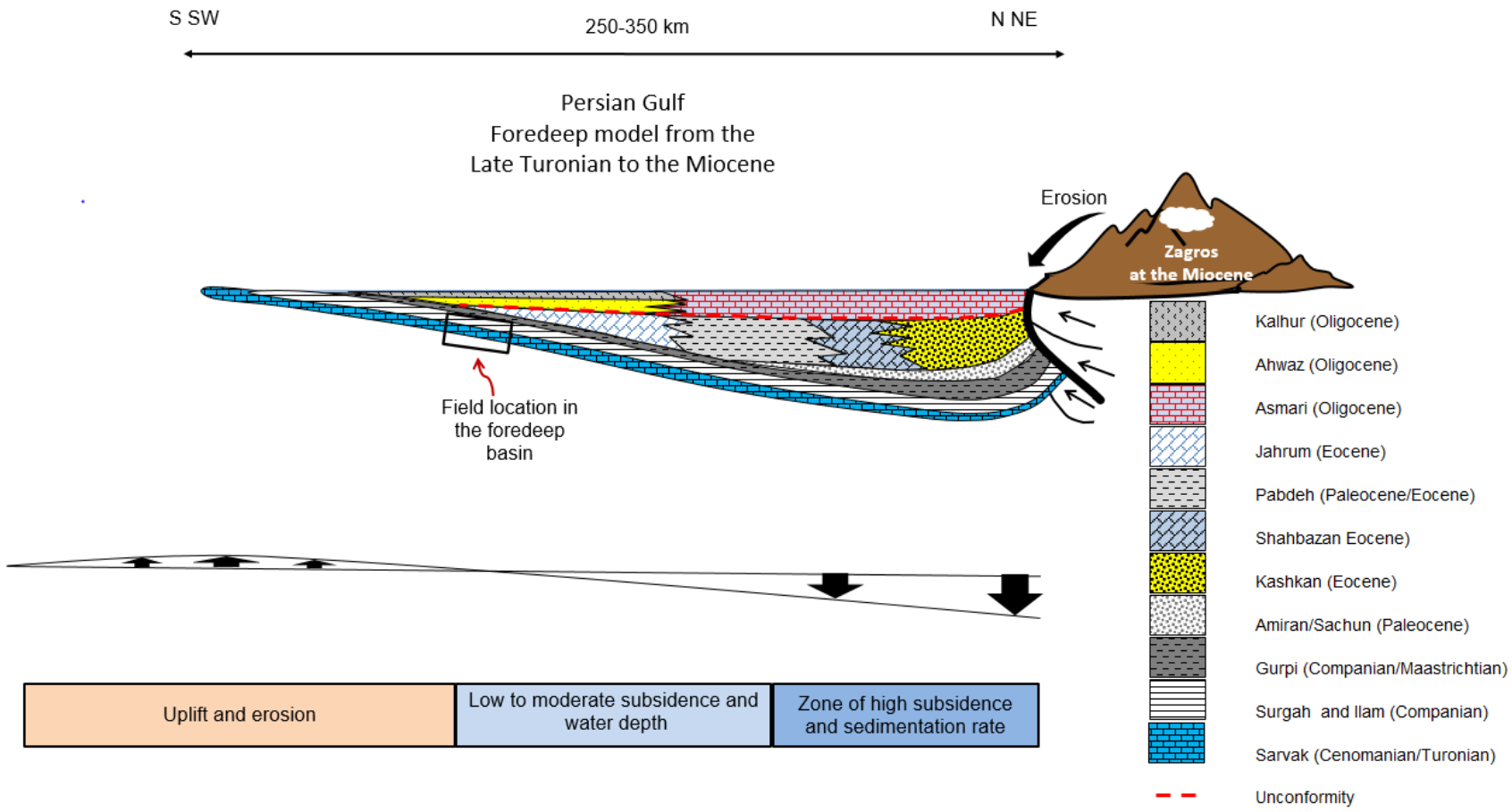

Figure 5: Sedimentation in the Persian Gulf foreland basin from the late Turonian to the Miocene. Location of field B on the basin is shown with rectangle.

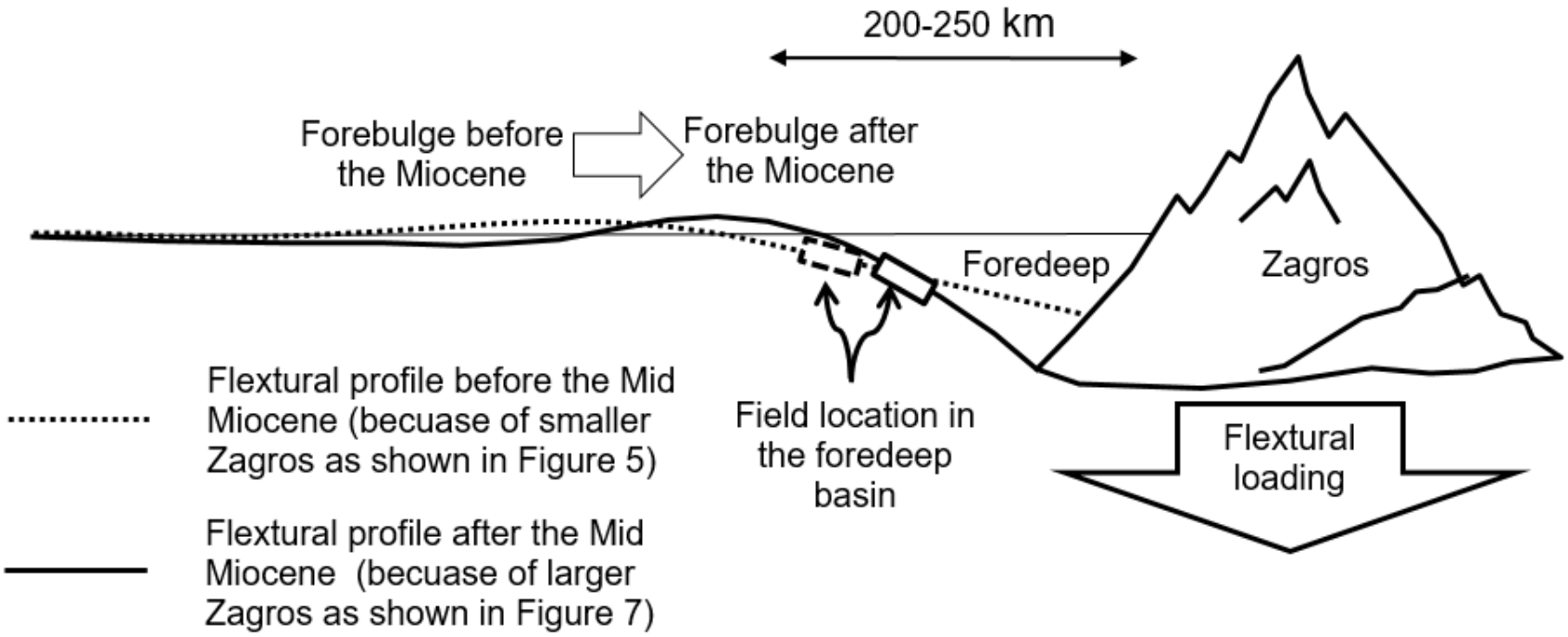

Figure 6: Movement of the Persian Gulf forebulge toward the orogenic suture making the Persian Gulf narrower after Mid Miocene. Locations of field B before and after tectonic subsidence is shown with dash and solid rectangles respectively. This exerted a northward tilting on the entire basin.

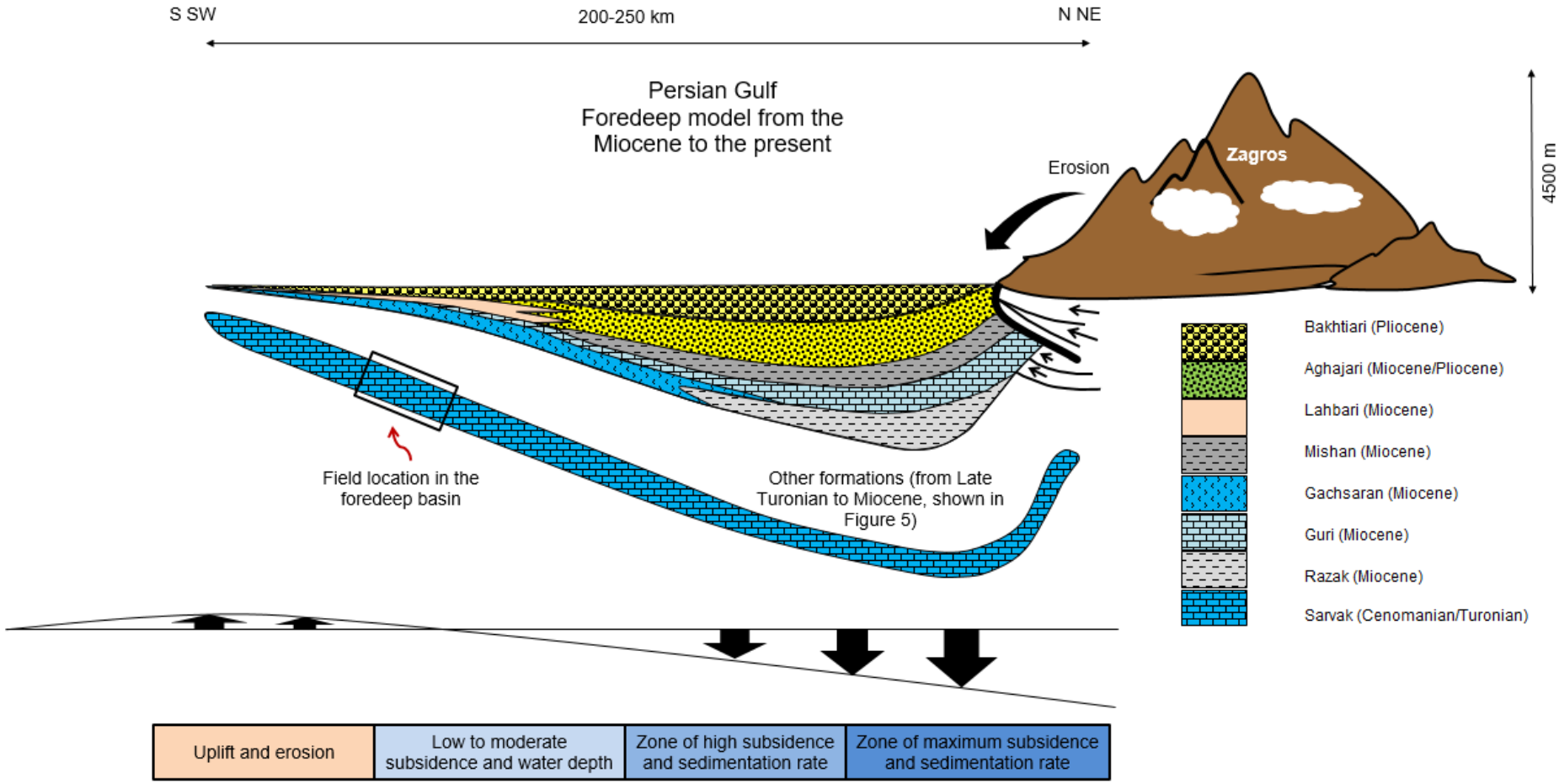

Figure 7: Sedimentation in the narrower and northwardly tilted Persian Gulf foreland basin from the Mid Miocene to the present. Location of field B on the basin (Sarvak Fm is the reservoir) is shown with rectangle.

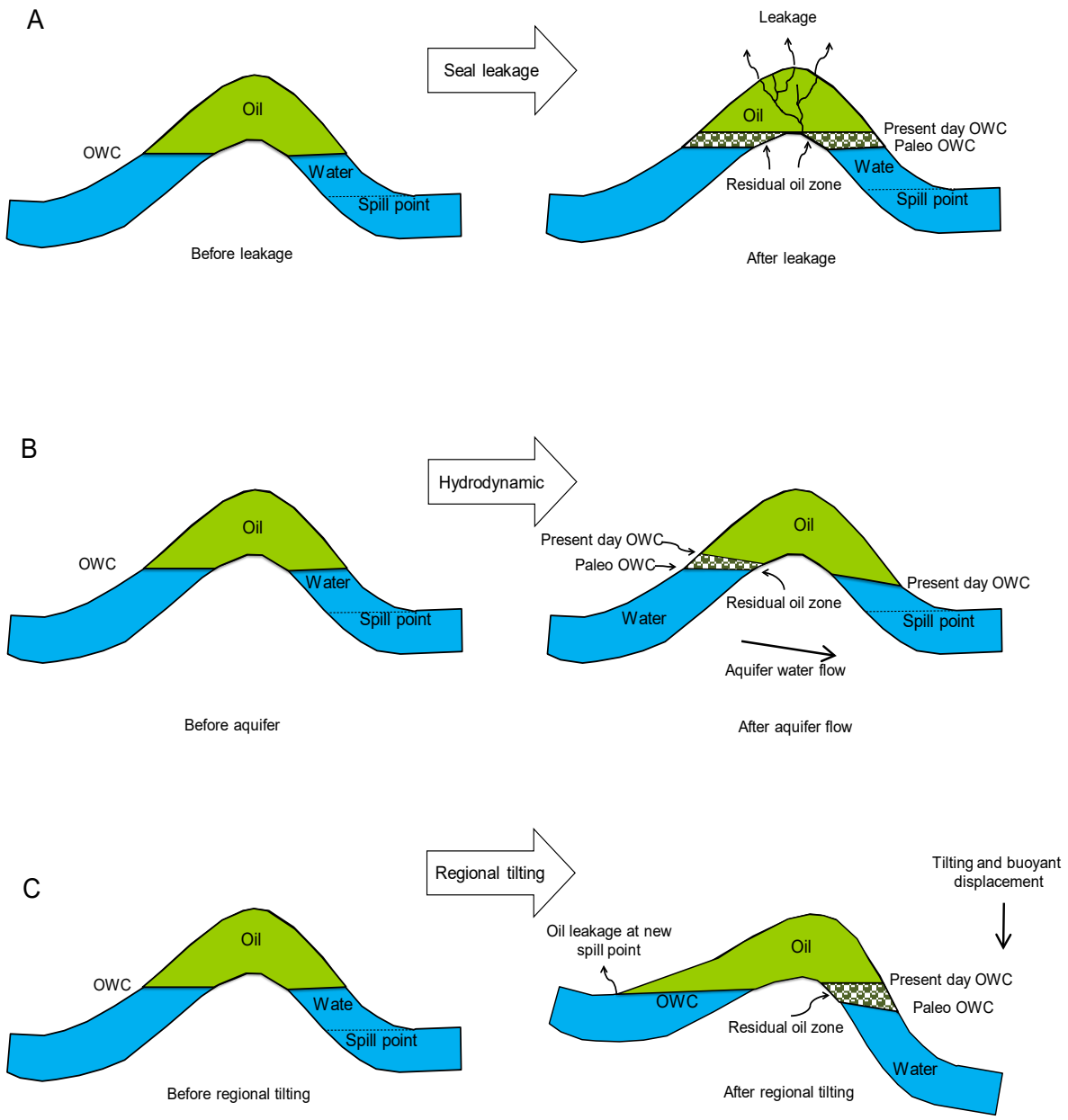

Figure 8: The most important processes of forming ROZ prior to the start of reservoir production. A: leakage in the seal and cap rock, B: hydrodynamic and active aquifer, C: regional tilting.

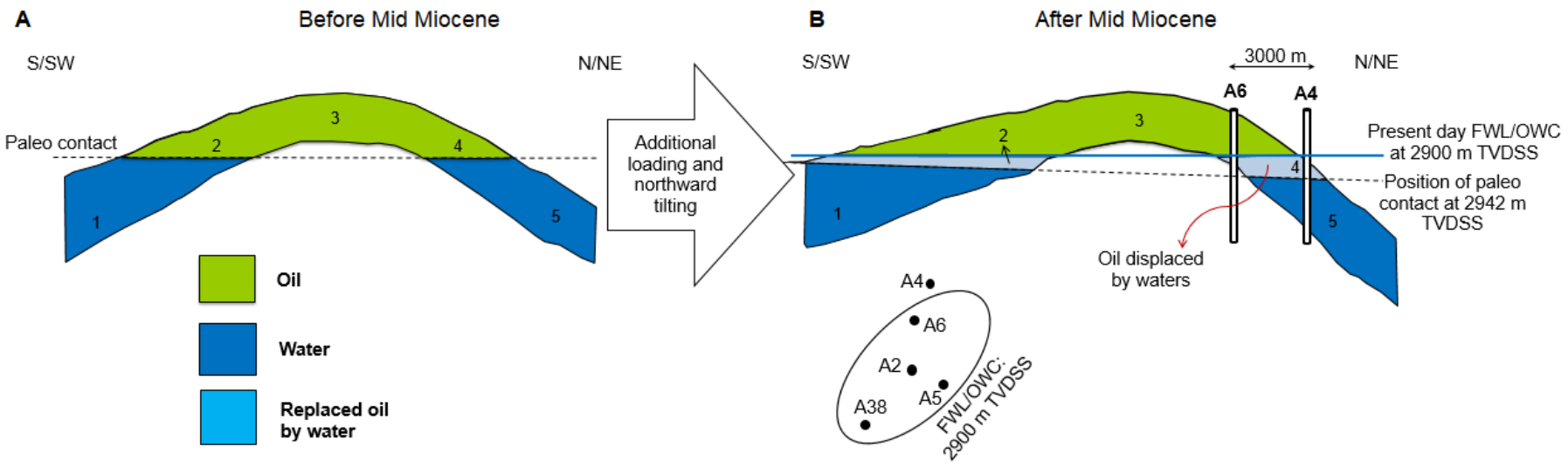

Figure 9: Effect of basin tilting on FWL and OWC adjustment and and changing capillary pressure regimes across the field A,

A: Before Mid Miocene, regions 1 and 5 were located below the fluid contact and other areas (2, 3 and 4) were above the fluid contact.

B: After Mid Miocene, regions 1, 2, 4 and 5 were located below the fluid contact and area 3 were above the fluid contact. Early accumulated oil in regions 2 and 4 was displaced by water and residual oil was trapped below the new fluid contact.

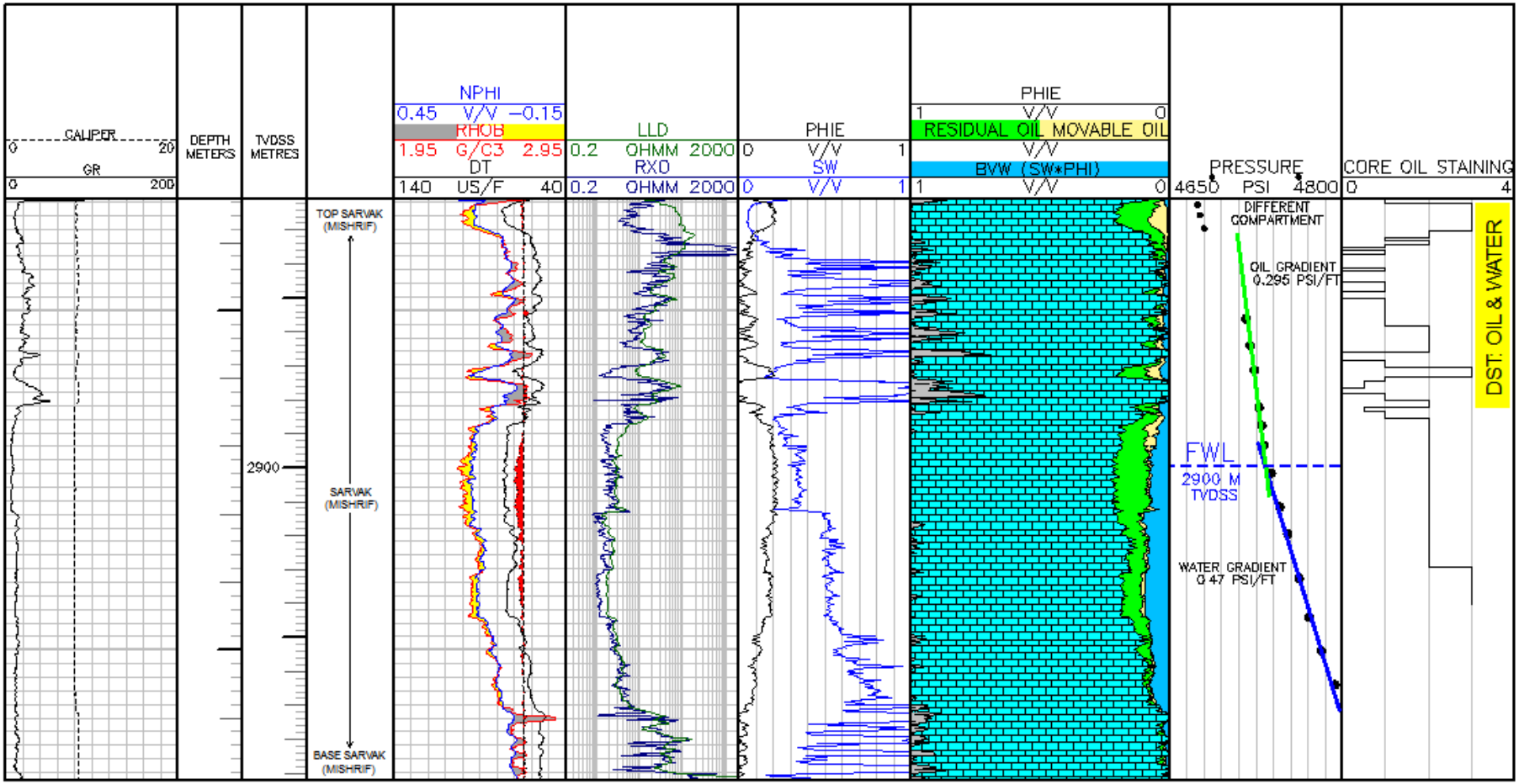

Figure 10: Petrophysical evaluation of A6 showing a FWL at 2900 TVDSS. There is a thickness of residual oil zone and oil staining below this FWL.

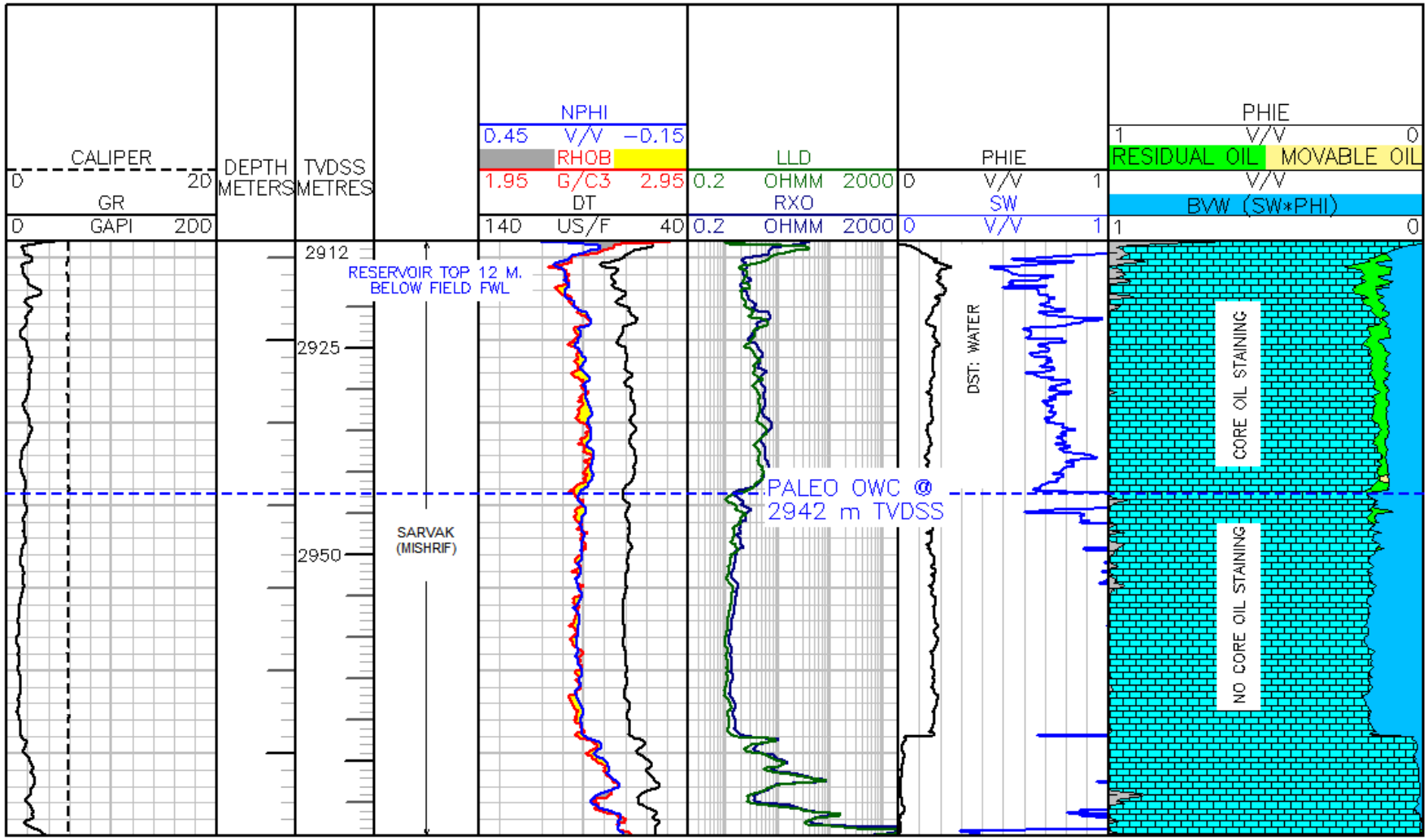

Figure 11: Petrophysical evaluation of well A4. This well was drilled on the northern flank of field A beyond the FWL (2900 m TVDSS). Top Sarvak (Mishrif) is located 12 m below the present day FWL. 30% residual oil below the field FWL and OWC disappears at 2942 showing a paleo fluid contact.

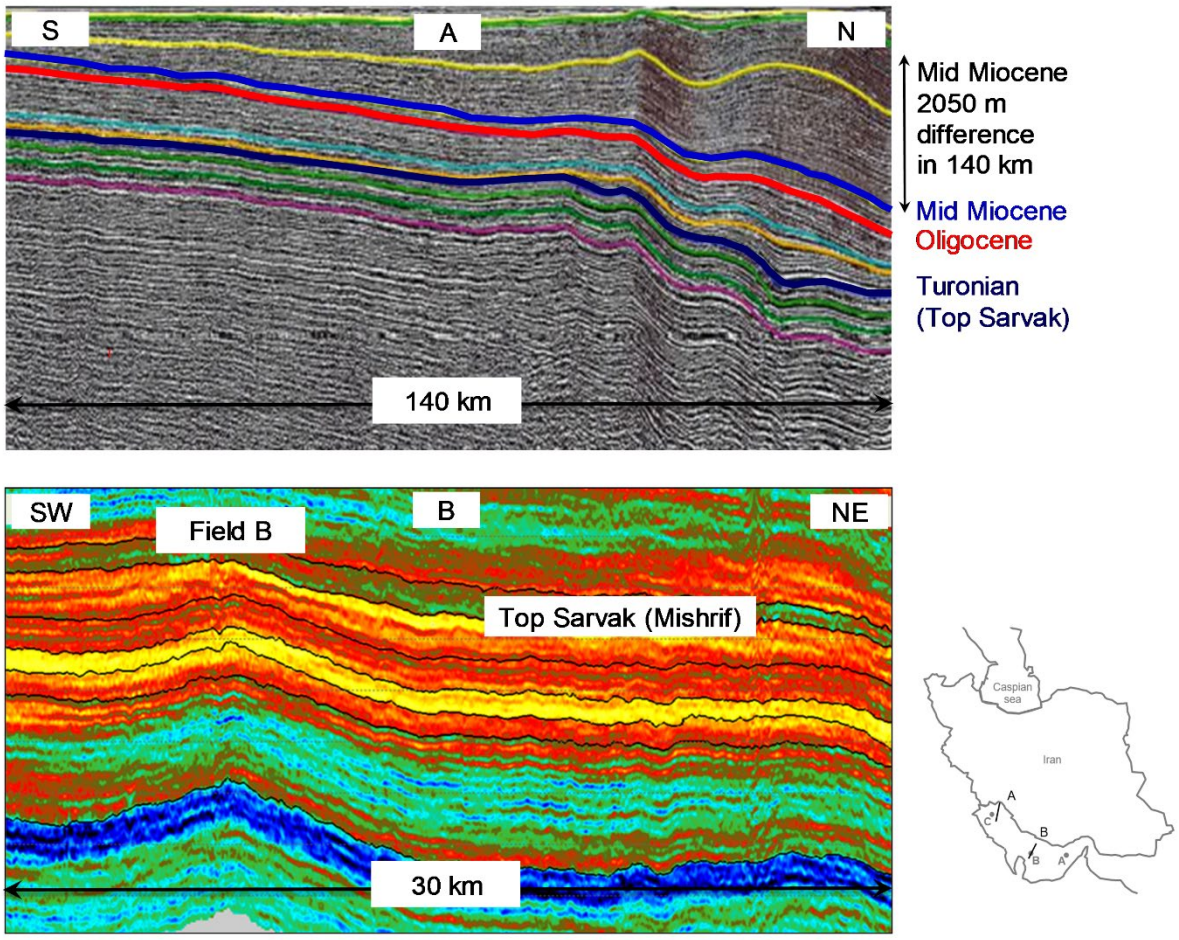

Figure 12: A: Long regional seismic section (140 km) crossing field A illustrates asymmetric and wedge-shaped Persian Gulf foreland basin. The Mid Miocene horizon shows a 2050 m flexural load over 140 km suggesting a tilt of 0.836 degrees for the Persian Gulf foreland basin.

B: Acoustic Impedance section through Field B emphasises same northwardly tilting.

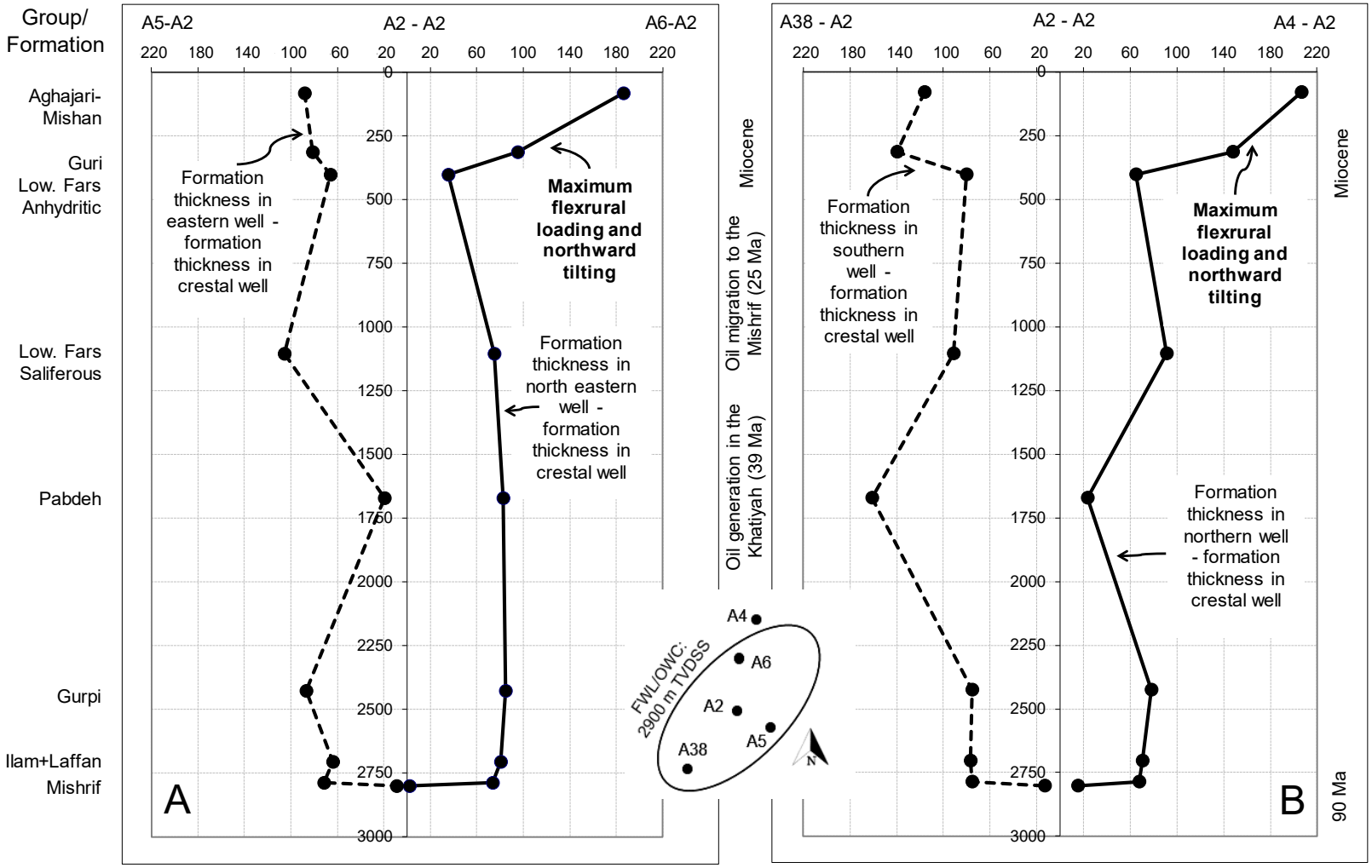

Figure 13: Thickness comparison and structural growth in one of the studied fields following deposition of the Sarvak (Mishriff) Fm reservoir. Both plots (A and B) show an increase in the thickness of formations deposited after the Miocene (Guri, Gachsaran, Mishan, Aghajari and

Bakhtiyari Formations) in the northern wells (A4 and A6) compared to central (A2) and southern wells (A5 and A38). This is related to additional tilting toward N and NW which was superimposed to the entire basin after Mid Miocene.

Graphic Abstract: Presence of residual oil below the present-day FWL is related to the north-east downward tilting of the entire Persian Gulf foreland basin

Figure 1: Examples of the presence of residual oil below the FWL and OWC in three studied fields (A, B and C). Second track shows fliud content: green =oil, blue =water. More residual oil below the FWL and OWC is seen in the northerrn parts of each field.

Figure 2: Cross plots of static formation pressure data vs depth (TVDSS). A) FWL at 2900 m TVDSS in field A and B) FWL at 2337 m TVDSS in field C.

Figure 3: Fluid contact (blue line) determination in wells drilled and logged prior to the start of production in studied fields. Field A presents a FWL obtained from the formation pressure data in a northern well. This FWL is supported by the same OWC depth determined from the log data in two southern and one northern wells. A paleo OWC is seen at 2942 m TVDSS.

Field B shows an OWC at 1221 m TVDSS from the data of 5 wells located in different parts of the field. There is no formation pressure data in this field.

Field C illustrates a FWL at 2337 m TVDSS determined from the extrapolation of formation pressure data in a well located in the south of the field. Depth of this FWL is supported by ODT and WUT seen in a well drilled on the northern flank of the field.

Figure 4: Summary of regional geology in the area.

Figure 5: Sedimentation in the Persian Gulf foreland basin from the late Turonian to the Miocene. Location of field B on the basin is shown with rectangle.

Figure 6: Movement of the Persian Gulf forebulge toward the orogenic suture making the Persian Gulf narrower after Mid Miocene. Locations of field B before and after tectonic subsidence is shown with dash and solid rectangles respectively. This exerted a northward tilting on the entire basin.

Figure 7: Sedimentation in the narrower and northwardly tilted Persian Gulf foreland basin from the Mid Miocene to the present. Location of field B on the basin (Sarvak Fm is the reservoir) is shown with rectangle.

Figure 8: The most important processes of forming ROZ prior to the start of reservoir production. A: leakage in the seal and cap rock, B: hydrodynamic and active aquifer, C: regional tilting.

Figure 9: Effect of basin tilting on FWL and OWC adjustment and and changing capillary pressure regimes across the field A,

A: Before Mid Miocene, regions 1 and 5 were located below the fluid contact and other areas (2, 3 and 4) were above the fluid contact.

B: After Mid Miocene, regions 1, 2, 4 and 5 were located below the fluid contact and area 3 were above the fluid contact. Early accumulated oil in regions 2 and 4 was displaced by water and residual oil was trapped below the new fluid contact.

Figure 10: Petrophysical evaluation of A6 showing a FWL at 2900 TVDSS. There is a thickness of residual oil zone and oil staining below this FWL.

Figure 11: Petrophysical evaluation of well A4. This well was drilled on the northern flank of field A beyond the FWL (2900 m TVDSS). Top Sarvak (Mishrif) is located 12 m below the present day FWL. 30% residual oil below the field FWL and OWC disappears at 2942 showing a paleo fluid contact.

Figure 12: A: Long regional seismic section (140 km) crossing field A illustrates asymmetric and wedge-shaped Persian Gulf foreland basin. The Mid Miocene horizon shows a 2050 m flexural load over 140 km suggesting a tilt of 0.836 degrees for the Persian Gulf foreland basin.

B: Acoustic Impedance section through Field B emphasises same northwardly tilting.

Figure 13: Thickness comparison and structural growth in one of the studied fields following deposition of the Sarvak (Mishriff) Fm reservoir. Both plots (A and B) show an increase in the thickness of formations deposited after the Miocene (Guri, Gachsaran, Mishan, Aghajari and Bakhtiyari Formations) in the northern wells (A4 and A6) compared to central (A2) and southern wells (A5 and A38). This is related to additional tilting toward N and NW which was superimposed to the entire basin after Mid Miocene.